A Study on the Tribological Performance of Nanolubricants

Yeoh Jun Jie Jason [1], Heoy Geok How [1,*], Yew Heng Teoh [2,*] and Hun Guan Chuah [1]

[1] Department of Engineering, School of Engineering, Computing and Built Environment,
   UOW Malaysia KDU Penang University College, 32 Jalan Anson, Georgetown 10400, Penang, Malaysia;
   jjason5831@gmail.com (Y.J.J.J.); hunguan.chuah@kdupg.edu.my (H.G.C.)

[2] School of Mechanical Engineering, Universiti Sains Malaysia, Engineering Campus,
   Nibong Tebal 14300, Penang, Malaysia

* Correspondence: heoygeok.how@kdupg.edu.my or howheoygeok@gmail.com (H.G.H.);
   yewhengteoh@usm.my or yewhengteoh@gmail.com (Y.H.T.)

Abstract: In recent years, the tribology field has expanded with the advent of nanolubrication. Nanolubricants are the name given to the dispersion of nanoparticles in a base oil, and has attracted researchers due to its potential application. In addition to being used in the tribology field, nanoparticles are also used for medical, space, and composites purposes. The addition of nanoparticles in base oils is promising because it enhances specific tribological characteristics including wear-resistance and friction, and the most important reason is that the majority of them are environmentally friendly. This paper reviews the tribological effect of various nanoparticles as lubricant additives. Parameters of nanoparticles that affect tribological performance, the technique to enhance stability, and lubrication mechanism that is currently believed to function will be delineated in detail. Moreover, this review facilitates an understanding of the role of various nanoparticles, which helps in developing and designing suitable nanolubricants for various applications.

Keywords: nanoparticles; nanolubricants; tribological performance; lubrication mechanism; dispersion stability

1. Introduction

Tribology is the study of science related to friction, wear, and lubrication [1]. Lubrication is the process or technique to reduce the friction and wear for two relative moving surfaces by using lubricant. The benefits provided by lubrication include rust, water, and dust prevention and as an insulator in transformer [2]. Wear and friction can cause machinery failure (for example in the engine, shaft, bearings, gears) and energy losses. Hence, it is essential to have sufficient lubrication to overcome these issues. Hence, it is essential to have sufficient lubrication to overcome these issues. An analysis by Holmberg et al. [3] conclude that friction in the engine and other moving parts can result in the waste of one third of all the fuel energy used. They also analyze new technology that can reduce friction by 18% over 5–10 years and a 61% reduction over 15–25 years for automobiles. Additionally, the potential techniques for friction reduction such as coatings and surface texturing on automobile parts, novel additives, reducing the width of tires had been suggested.

Moreover, lubricant is an indispensable tool which is used to lubricate machinery to protect operating mechanical parts from wear and reduce friction. Mineral oil as a lubricant has already been in use for a long time. However, pollution in aquatic and terrestrial ecosystems caused by the disposal of mineral oil directly affected the environment [4]. An alternative source such as biolubricant oil is a promising replacement to mineral oil because it is biodegradable and nontoxic. Further, biolubricants

evidence several advantages compared to mineral oil including excellent lubricity, obtaining high flash point, viscosity, and low volatility.

To further minimize wear and friction in the system, small amounts of weight percentage of additives are added to the lubricant base stock to improve and enhance the oil properties. Those additives can be anti-wear (AW), extreme pressure (EP), anti-corrosion, dispersant, and AW and EP additives are especially used to lubricate mechanical parts. One should note that the traditional EP and AW additives are chlorine and phosphorus compounds, which have been restricted in terms of use due to the purpose of environment protection. To overcome this problem and most of the existing lubricants which have reached performance bottlenecks, researchers are currently investigating nanoparticles (NPs) design as a new class of lubricant additives. Most NPs are environmentally friendly and exhibit tribological properties improvement in lubricants since it does not require trioactive elements such as chlorine, phosphorus, and sulphur, which are harmful to the environment [5,6]. Moreover, the nanometer size range of NPs are able to fill contact asperities. They function as AW and EP additives and friction modifiers, obtain high thermal stability, and react with the friction surface without an induction period [7].

To date, various type of NPs used as lubricant additives have been documented in many studies. Metal [8], metal sulphides [9], metal oxide [10], boron nitrides [11], carbon materials [12,13], nanocomposites [14], and rare earth compounds [15] exhibit excellent wear and friction reduction. In this present study, NPs as lubricant additives will be reviewed. This review including the experiment test condition (speed, time, temperature, tested stock), NP information (size, concentration), the optimum concentration of NPs, the dispersion method, the method to evaluate dispersion stability, the lubrication mechanism of NPs, and the parameters of NPs that affect tribological properties in the lubricant. The relevant tribology information regarding the lubricants will also be discussed.

2. Tribology

Tribology is the study of the science of interacting surfaces or two moving bodies in relative motion. It is related to friction, wear, lubrication, degradation of metal surfaces, corrosion, engine life, and energy losses. Since there are incredibly high energy losses due to this phenomenon, such losses caused by friction and wear should be minimized [16]. To satisfy the lubrication requirements of the particular application, specifically in tribological aspects, the most important way is selecting a suitable lubricant. Lubrication, friction, and wear are related to tribological performance. Lubricity is concerned with the formation of a protective layer or tribofilm on the contact surfaces. High lubricity reduces direct surface contact, thereby reducing friction and energy losses [17]. However, having a high lubricity is not always accompanied by better wear protection, because the formation of a protective layer on the rubbing surfaces happens through the absorption of the surface-active substance of lubricants such as base stocks or additives. When surface asperity contacts each other, three types of mechanical wear are possible resulting in the following: adhesion, abrasion, and fatigue [18]. Adhesive wear occurs when high loads, high temperature, or inadequate lubrication cause two relatively moving surfaces asperity welds and then immediately tear apart. Abrasive wear happens when surface rubbing occurs between contact surfaces of relative hardness. Fatigue wear is the progressive and localized structural damage of material in repeated loading [19]. Prior to discussing the tribological performance of the nanolubricants, it is necessary to understand the three basic tribology parameters, which are the mechanical properties of a tribological system, lubrication, and the physicochemical properties of the lubricant [19].

2.1. Energy Losses

Energy losses due to friction are incredibly high. Energy losses in the engine due to friction result in heating and promote the wear on the surfaces of moving part. It has been reported that 75–82% total energy losses in the vehicle, engine losses is between 68% and 72%, 12–30% energy from fuel used to move the vehicle and energy losses due to friction are around 3%, as shown in Figure 1 [20,21].

The combined effect of friction and wear caused 30% total energy losses [22]. Energy losses due to the friction can be reduced by a few technologies such as the design of tires and bearings, tribology, and additives. Further, in order to overcome the energy losses, the lubricant which imparts the best lubrication is essential.
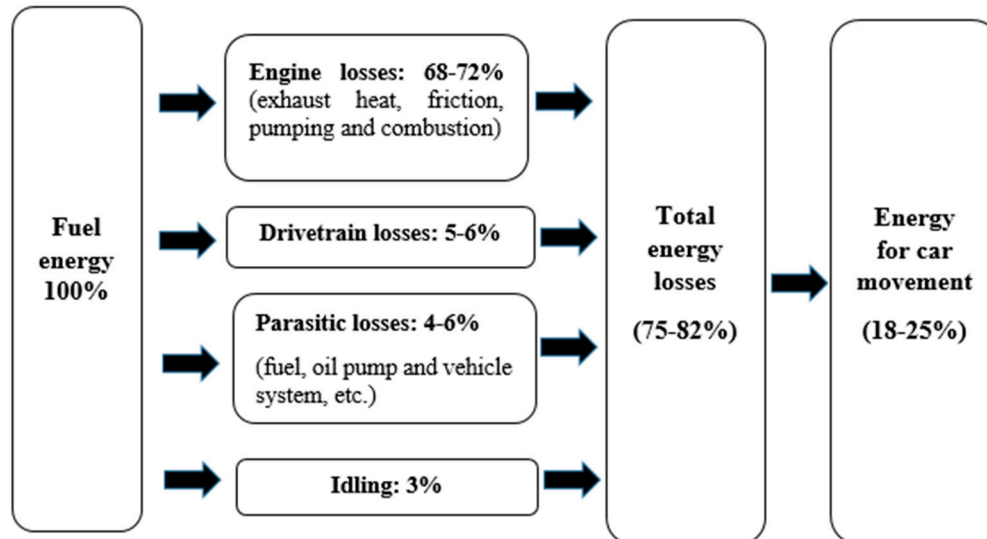

Figure 1. Energy losses in an automobile [20,21]. "Adapted with permission from US Government, Where the Energy Goes: Gasoline Vehicle and the permission from Jordan Hanania, Energy losses".

2.2. Mechanical Properties of a Tribological System

The mechanical properties of a tribological system are related to material hardness and its surface roughness, contact geometry, and the sliding mechanism of the rubbing part, as shown in Figure 2. Discussion of those properties are limited to the laboratory tribometer. Usually, the material used for the test has a hardness of around 30-64 Hardness Rcokwell C (HRC) and 0.01–1.0 µm surface roughness. For example, the hardness and surface roughness of steel ball used in a four-ball tribometer is 62 HRC and 0.040 µm [23]. However, it still depends on the type of material, hardening process, and coating. Basically, the higher the hardness of materials, the more significant the wear resistance, while the lower surface roughness of materials evidences better lubricity [24]. It seems impossible to compare the tribological results between different types of tribometers, such as four-ball tribotester, pin-on-disk, ball-on-disk. This is because of varying sliding geometries and their sliding mechanism, for example, sliding and rolling. Some commonly used tribological test geometry configurations are shown in Figure 3. Valid comparisons can be achieved when conducted using a similar type of tribometer and method/parameter, for example, ASTM D2266, ASTM D2783, ASTM G99 [19].
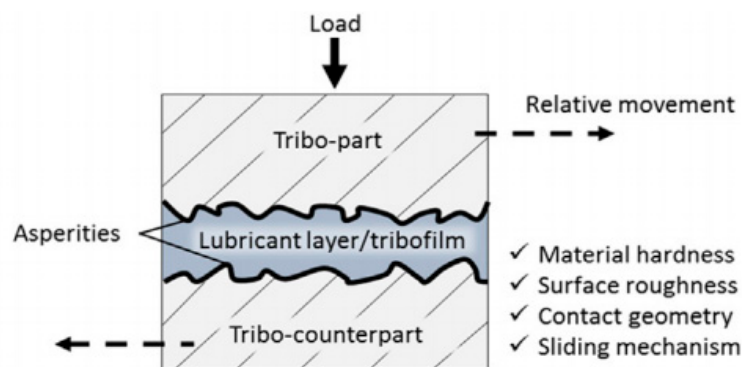

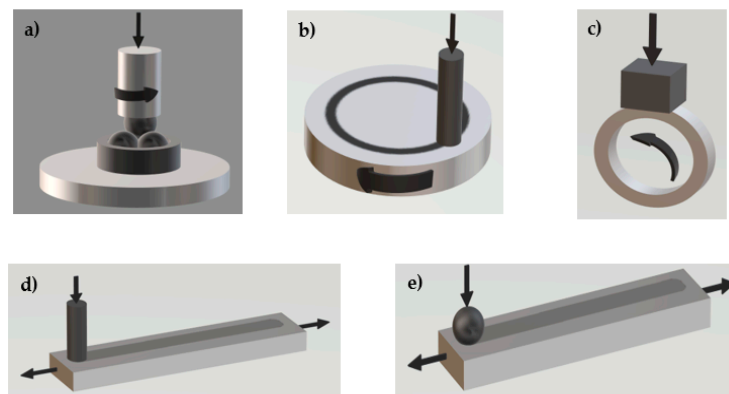**Figure 2.** Mechanical properties of a tribological system [19].

Figure 3. Commonly used tribological test geometry configuration: (**a**) four-ball tribometer, (**b**) pin-on-disc, (**c**) block-on-ring, (**d**) pin-on-flat, and (**e**) ball-on-flat.

2.3. Lubrication

Lubrication is essential to overcome and reduce friction between two interacting parts. According to the Stribeck curve, there are three well known lubrication regimes. The first regime is boundary lubrication (BL), second regime is mixed and elastohydrodynamic lubrication (EHL), and the third regime is hydrodynamic lubrication (HL) [25], as shown in Figure 4. BL happens when repeated loading/high load or low sliding speed generates heat and causes high wear and energy losses because of the unstable and thin tribofilm that forms on the rubbing surfaces. Thus, lubricant additives are important to protect the friction surface(s) [26]. Shock loading is also a factor that results in BL. Again, by further decreasing the load or increasing sliding speed, the lubrication regimes will shift to a mixed/EHL regime and then to a hydrodynamic regime. Through this transition, friction and wear will decrease due to hydrodynamic lift since a thicker tribofilm will separate the contacting surfaces. HL will occur when two interacting surfaces are separated by a tribofilm. In this regime, no significant mechanical wear occurs except fatigue due to the contacts being fully lubricated and the friction dominated by viscous dragging forces [26]. EHL is similar to hydrodynamic lubrication, but this lubrication is involved in the rolling motion. Mixed lubrication is a combination of BL and HL. When under a mixed/EHL regime, the tribofilm had around 1–3 times greater film thickness than surface roughness. Under the hydrodynamic regime, the tribofilm had three times greater film thickness than surface roughness [27]. Besides, the tribofilm in EHL lubrication is much thinner and the pressure exerted is greater than hydrodynamic lubrication. Typically, the coefficient of friction (COF) value of BL will greater than 0.1, while for mixed/EHL lubrication has a range of 0.01–0.10 COF and HL has a COF less than 0.01 [18].
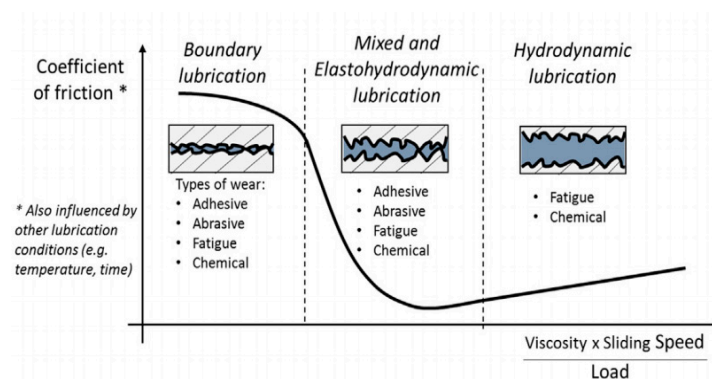

Figure 4. Graphical illustration of various types of lubrication regimes and conditions [19].

2.4. Physicochemical Properties of the Lubricant

One of the critical parameters for tribological performance is the physicochemical properties of the lubricant. Different types of oil have their properties, such as different viscosity, density, and flash point since they are made from the different feedstock. Viscosity indicates resistance to flow due to internal friction, and it is the most important property in lubricant oil. Furthermore, it is related to temperature, pressure, and the form of tribofilm, and ultimately decides the tribological performance [2]. Higher viscosity indicates higher flow resistance; increasing the viscosity of the lubricant creates a thicker tribofilm but provides lower efficiency due to higher viscosity results in more poor fuel atomization [28]. Considering the condition of temperature elevation and high loading, a lubricant that has a high pressure-viscosity coefficient and high viscosity index will be preferred, to ensure the tribofilm is stable. Other physical properties including pour point, flash and fire point, oxidative stability, and thermal stability will affect the strength and stability of the tribofilm [28].

Furthermore, the tribochemical characteristics of lubricants concern so-called surface active materials exhibit lubricity, load carrying capacity, and wear resistance. They primarily act as an anti-wear additive (AW), an extreme pressure additive (EP), and a friction modifier (FM) [19]. AW and EP additive are categorized into two main types, active and non-active. Active additives through the tribochemical reaction with the contact surface form a sacrificial protective film to reduce wear. In contrast, non-active additives form a protective film by becoming deposited via by-product to minimize wear. AW and EP additive have a similar function in terms of application. However, the difference between them is the rate of reaction of EP to form the protective film is higher, the film is more robust and thicker and suitable for high-speed operation. FM provides a softer, easily sheared protective film which minimizes light surface contacts (sliding and rolling friction), and thus less energy is consumed. Typically, the COF of FM film is 0.01–0.05, which is lower than COF of EP and AW film (0.06-0.15), but higher than the COF of EP and AW (0.001–0.009) under hydrodynamic regime [29]. Those additives mostly operate in BL and mixed/EHL lubrication regime, which result in protecting material surfaces and enhancing lubricity [19].

3. Nanolubricants and Base Oils

3.1. Nanolubricants

From here the use of nanoparticles/nanomaterials as lubricant additives are known as nanolubricants. Typically, their diameter particle size is between 1 and 100 nm. In laboratory tests, the use of nanolubricants in base oils or coatings promotes a significant reduction of friction and wear, which exhibits interesting tribological properties. Nanolubricants can be synthesized by the one-step method or two-step method. For the one-step method, the nanolubricants directly formulate through a chemical process. In the two-step method, the first procedure is the nanomaterials are synthesized in dry powder form by either physical or chemical methods, and the second procedure is to disperse them into base oil by mixing techniques with or without dispersants or surfactants [30]. An illustration of nanolubricants synthesis is shown in Figure 5.
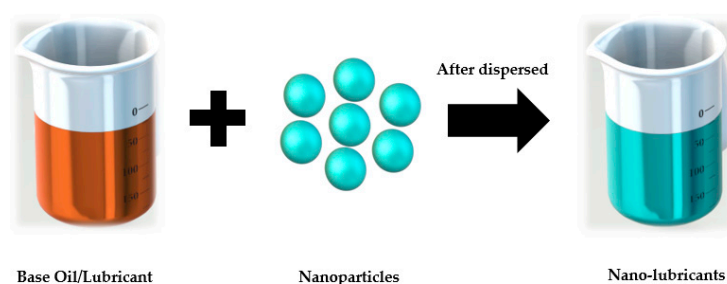

Figure 5. Synthesis of nanolubricants.

3.2. Base Oils

Lubricants are classified into three physical appearances: solid, semisolid, and liquid form. Generally, lubricants are synthesized from three different types of base oils. They are mineral oil, synthetic oil, and biolubricant. The American Petroleum Institute (API) classified lubricant base oil quality and the necessary information of different groups of base oils under API 1509, as shown in Table 1 [31]. Groups I–III base oils are refined from crude oil. Group IV base oils are fully synthetic oils made by polyalphaolefins (PAO). Group V base oils are those oils not found in groups I–IV categories. This group includes other base oils such as silicone, organophospahtes, polyalkyleneglycol (PAG), polyolester, and biolubricants.

Table 1. American Petroleum Institute base oil classification [31].

Base Oil Category	Properties		
	Sulfur (%)	Saturates (%)	Viscosity Index
Group I (solvent refined) *	>0.03 and/or <90		80 to 120
Group II (hydrotreated) *	<0.03 and >90		80 to 120
Group III (hydrocracked) *	<0.03 and >90		>120
Group IV **	Polyalphaolefins (PAO) synthetic lubricants		
Group V	All other base oils not included in Group I to IV		

Noted: * is in the mineral oil category, ** is in the synthetic oil category.

Mineral oil is refined from crude oil by fraction distillation. The chemical composition of mineral oil is classified into paraffinic, naphthenic, and aromatic. Paraffinic contains primarily paraffin straight-chain hydrocarbon, naphthenic hydrocarbons are in the cyclic structures with no unsaturated bonds, and aromatic hydrocarbon also has a cyclic structure derived from benzene [32,33]. Mineral oil is the economic base oil and also serves as a common lubricant widely used in industry but harms both the environment and health. Typically, they are used in engines, gears, and bearings, etc.

Synthetic oil is artificially made from hydrocarbons or other chemicals. This lubricant can be manufactured by chemically modifying petroleum products instead of using whole crude oil. The formulation of synthetic oil provides superior properties over mineral oils, including the ability to lubricate in extremely low or high temperatures and offers better wear protection [33]. In addition, synthetic oils also provide several economic benefits including reducing energy consumption and maintenance costs, and improving energy efficiency, etc. Additionally, synthetic lubricants are designed to fulfil the high demands of modern machinery [34]. Conversely, a few synthetic oils may also cause harm to the environment [35].

Biolubricant is mainly made from vegetable oils such as sunflower, coconut, Jatropha, rapeseed, and palm while fusel oil is also acceptable for biolubricant production. Synthetic esters and petroleum products that fulfil biodegradability and toxicity criteria can also be used to manufacture biolubricants [2]. Biolubricant base stocks are the primary factor that decides the properties of biolubricants. The properties include physicochemical properties, renewability, and degradability. Among these properties, tribological properties are the most critical criterion. Moreover, biolubricants are an alternative source due to their widespread sources, and they are also renewable, biodegradable, and eco-friendly. Biolubricants offer several advantages over mineral oil, and it has high lubricity, high viscosity index, high flash point, low volatility, and high dispersion [36,37].

4. Various Types of Nanoparticles as Lubricant Additives

Based on the chemical composition, nanoparticles consist of metal, metal oxide, sulphide, nanocomposites, carbon nanoparticle, and rare earth compounds. According to Dai et al. [38], metal-containing nanoparticles are the subject of most of the studies carried out, and they occupy 72% of the reviews. In contrast, studies that focused on carbon nanoparticles, nanocomposites, and rare earth compounds accounted for just 7%, 6%, and 7%, respectively.

4.1. Metal

Form here the metallic NPs have a small particle size, high surface area, low melting point, and low shear strength. They provide excellent tribological performance and self-repairing function as lubricant additives [39], including Cu, Bi, Sn, Fe, Ni, Al, Pd, Co, Zn. The lubrication mechanism of metallic NPs can be categorized into (a) the surface properties will be changed and separate two friction surfaces with the formation of tribofilms, hence provide promising tribological performance; (b) NPs roll between two friction surface leading to the reduction of friction and wear; (c) heat and pressure generated during operation, leading to the compaction of NPs on the wear track, with this phenomenon considered as a repair or sintering effect [38].

Padgurskas et al. [40] investigated the tribological properties of Fe, Cu, and Co NPs and their mixture as lubricant additives on SAE 10 mineral oil. They reported that the use of nanoCu is the most effective NPs to reduce friction and wear both alone or as a mixture, and the mixture of NPs is more effective than pure NPs. Asadauskas et al. [41] conducted a comparative study of tribological properties of Cu, Fe, and Zn NPs between vegetable oil (rapeseed oil, soy oil, canola oil, and olive oil), mineral oil, and synthetic oil. They reported that without NPs, synthetic oil obtained the lowest wear, and with the addition of NPs, nanoFe evidenced better dispersion stability than nanoCu and nanoZn. NanoFe improved the wear resistance of rapeseed oil, while nanoZn reduced wear and smoothened scars in mineral oil.

The addition of nano-bismuth in light and heavy base oil resulted in wear reduction from 535 to 454 μm and 651 to 563 μm, friction reduction from 0.091 to 0.052 and 0.074 to 0.047 [42]. The addition of nanoCu in paraffin oil resulted in a reduction of friction (23%) and wear (26%) [39]. An investigation of the tribological properties of nanoNi in PAO6 reported a reduction of 7–30% in wear and 5–45% in friction [43]. Furthermore, the addition of nanoAl increased load carrying capacity and improved friction and wear [44]. The summary of literature for metallic NPs as lubricant additives is shown in Table 2.

Table 2. Summary of literature for metallic nanoparticles as lubricant additives.

Details of Nanolubricant				Dispersion Method, Duration & Temperature	Tribometer	Test Parameters			Test Results		Optimum Conc.	Ref.
Nanoparticle	Base Oil	Particle Size	Conc.			Load	Speed	Temp. & Duration	Wear Reduction	Friction Reduction		
Category: Mineral oil												
Bi	Light base oil	7–65 nm	900 mg/L	Magnetic stirrer, 30–40 min, <80 °C	Four ball tester	392 N	1200 rpm	75 °C, 30 min	From 535 to 454 µm	From 0.091 to 0.052	-	[42]
	Heavy base oil		310 mg/L						From 651 to 563 µm	From 0.074 to 0.047		
Cu	Paraffin Oil	10–60 nm	0.02 wt%	-	Four ball machine	300 N	1450 rpm	20 °C, 30 min	Reduction of 23%	Reduction of 26%	0.02 wt%	[39]
	Chevron Taro 30 DP 40 and Teboil Ward	80–120 nm	3 wt%	-	Pin-on-disk tribometer	0.1–180 mN	0.02 mm/s	25 °C	From 0.023 to 0.018 mg	From 0.15 to 0.11	3 wt%	[45]
	SAE grade 15W-40	50 nm	2.5, 5, 7.5 and 10 wt%	Mechanical agitation & ultrasonic dispersion, 30 min	Ball-on-disk tribometer	50 N	10 to 30 Hz	Rt, 30 min	The wear reduced as the concentration increase until 10 wt% wear increase		7.5 wt%	[46]
Al	Paraffin Oil	65 nm	0.025–5 wt%	Ultrasonic stirring, 30 min	Ball-on-ring tester	50–300 N	500 rpm	Rt, 1 h	Addition of Al increase load carrying capacity and improve friction and wear		0.5 wt%	[44]
Fe, Cu, Co	SAE 10 mineral oil	-	0.5 wt%	-	Four ball tribotester	150 N	1420 min^{-1}	-, 1 h	Reduce up to 11% (Co), 23% (Fe), 47% (Cu)	Reduce up to 20% (Co), 39% (Fe), 49% (Cu)	0.5 wt%	[40]
Category: Synthetic oil												
Ni	Polyalphaolfin (PAO6)	20 nm	0.5, 1.0, 2.0 wt%	Ultrasonic probe, 30 min	Block on ring, four ball tester	165 N, -	2 m/s, 1470 rpm	-	Reduction between 7–30%	Reduction between 5–45%	0.5 wt%	[43]
		7.5, 13.5 and 28.5 nm	0.02, 0.05, 0.1, 0.2, 0.4 wt%	-	Four ball friction and wear tester	300 N	1450 rpm	-, 30 min	Addition of 0.05 wt% Ni exhibit excellent anti wear behaviour		0.05 wt%	[47]
Cu	Polyalphaolfin (PAO6)	25 nm	0.5 and 2 wt%	Ultrasonic probe, 30 min	Block and ring, four ball tester	165 N, medium load	1 m/s, 1470 rpm	-	Reduction of 50% wear for 0.5 wt% and reduction of 16% wear for 2 wt%		0.5 wt%	[48]
Category: Biolubricants												
Cu	Pongamia Oil	25–85 nm	0.025, 0.05, 0.075 & 0.1%	Ultrasonicator	Pin-on-disk tribometer	40 N	200 to 800 rpm	-	Only addition of 1% nano-copper cause the further increase of wear and COF		0.075 wt%	[49]
Category: Others/none												
Cu	-	24 nm	0.01, 0.05, 0.1, 0.2, 1.0 wt%	-	Ball-on-disc tribotester	50 N	0.2 m/s	Rt	Improved 1.57 times	Improve by 27.6%	0.05 wt%	[50]
	Lithium grease	50–100 nm	0.2, 0.5, 1.0, 2.0 wt%	Homogenized by triple-roller mill	Ball-on-disk tribometer	200 N	50 Hz	80 °C, 2 h	Reduction of 82.2% wear loss	Reduction of 12% friction	0.5 wt%	[51]
Sn & Fe	Macs base oil	30–60 nm & 20–70 nm	0.1, 0.5, 1.0 wt%	Ultrasonic probe, 5 min	Vacuum four ball tribometer	300 N	1450 rpm	25 °C, 30 min	Sn and Fe exhibited friction and wear reduction, but Sn effective on friction reduction and Fe effective on anti-wear		1.0 wt%	[52]
Pd	TBA	2 nm	1–10 wt%	-	Ball-on-disc tribometer	1–20 N	10 cm/s	-	Addition of 2 wt% of Pd improve the tribological properties, above 5 wt% wear rate increase		2.0 wt%	[53]

4.2. Metal Oxide

Various metal oxides have been used as lubricant additives, including TiO_2, CuO, ZnO, Al_2O_3, Fe_3O_4, $ZnAl_2O_4$. The lubrication mechanism of metal oxide NPs is similar to the metallic NPs, including rolling effect, sintering and repair effect, and tribofilm formation.

Alves et al. [54] studied the tribological behavior of ZnO and CuO in vegetable oil (sunflower and soybean), synthetic oil, and mineral oil. They found that the addition of CuO in synthetic oil improves tribological properties, ZnO mineral-based lubricants exhibit excellent friction and wear reduction, while the addition of NPs in vegetable oil were not beneficial for wear reduction. The addition of TiO_2 in water-based lubricant exhibits excellent tribological performance [55,56], while in engine oil SAE 20W 40, wear showed significant reduction and friction reduced by 50% [57]. Luo et al. [58] investigated the tribological properties of Al_2O_3 in pure lubricating oil with two types of tribometer. They reported that through the four-ball tribometer, the average coefficient of friction (COF) reduction is 17.61% and 41.75% reduction for wear scar diameter (WSD). Friction is reduced by 23.92% by using a thurst-ring tribometer. This is because of the formation of a protective film on the contact surface and rolling effect. One should note, however, that the addition of Al_2O_3 had a detrimental impact on PAO and SAE75W-85 [59]. Typical studies of metal oxides as lubricant additives are set out in Table 3.

Table 3. Summary of literature for metal oxide nanoparticles as lubricant additives.

Nanoparticle	Base Oil	Particle Size	Conc.	Dispersion Method, Duration & Temperature	Tribometer	Load	Speed	Temp. & Duration	Wear Reduction	Friction Reduction	Optimum Conc.	Ref.
	Details of Nanolubricant					Test Parameters			Test Results			
Category: Mineral oil												
Al_2O_3	Pure lubricating oil	78 nm	0.05, 0.1, 0.5, 1.0 wt%	Ultrasonication, 30 min	Four ball tribometer, thrust-ring tribometer	147 N, 200 N	1450 rpm, 1200 rpm	75 °C, 30 min	Average COF reduction are 17.61% (four ball) and 23.92% (thurst-ring), WSD reduction of four ball test is 41.75%		0.1 wt%	[58]
TiO_2	Mineral oil	20–25 nm	0.25, 1, 2 wt%	Mechanical stirrer, 15 min	Reciprocating pin-on-disk	14.715 N	0.05 m/s	Ambient, 30 min	Reduction of 0.01 COF		0.25 wt%	[60]
	Multi-grade engine oil SAE 20W 40	10–25 nm	1.5 wt%	Ultrasonic shaker	Pin-on-disc tribometer	40, 60, 90 N	0.5, 1.0, 1.5 m/s	-, 5 min	Wear significant reduce	Reduced by 50%	1.5 wt%	[57]
CuO	Mineral oil	30–40 nm	0.5–1.5 wt%	Ultrasonic shaker, 30 min	Pin-on-disc tester	40 & 60 N	0.5–1.5 m/s	-	Wear significant reduce	Reduce up to 50% of COF	1 wt%	[61]
	Paraffin oil	50 nm	0.2, 0.25, 2 & 3 wt%	Ultrasonic bath, 1 h	Four-ball tribomachine	40 kg	1200 rpm	60–70 °C, 15 min	The higher the concentration of CuO, the better the tribological properties		-	[62]
$ZnAl_2O_4$	Pure lubricant oil	95 nm	0.05, 0.1, 0.5, 1 wt%	-	Four ball tribometer, thrust-ring tribometer	147, 200 N	1450 rpm, 1200 rpm	348 K, 1800 s	Reduce up to 31.15%	Reduce up to 33.67%	0.1 wt%	[63]
Category: Biolubricants												
TiO_2	Trimethylolpropane (TMP) ester	-	1 wt%	Ultrasonic bath, 8 h	Four ball wear tester	40–120 kg	1200 rpm	Rt, 10 min	Decreased by 11%	Decreased by 15%	1 wt%	[64]
	Palm oil	22.98 nm	0.05, 0.1, 0.2 wt%	Ultrasonic bath, 30 min	Four ball tribotester	40 kg	1200 rpm	60–70 °C, 15 min	Only addition of 0.1 wt% TiO_2 exhibit reduction of friction and wear		0.1 wt%	[65]
CuO	Palm kernel oil (PKO)	40 nm	0.34 wt%	High-shear homogeniser, 40 min	Pin-on-disc tribometer	9.81 N	0.2 m/s	-, 60 min	Reducing the WSD by 48%	Reducing the COF by 56%	0.34 wt%	[66]
Category: Various test oil/others												
CuO & ZnO	Mineral oil, synthetic oil (PAO), sunflower oil, soybean oil	4.35 & 11.71 nm	0.5 wt%	Ultrasonic probe, 30 min	High frequency reciprocating test rig (HFRR)	10 N	20 Hz	50 °C, 60 min	CuO in synthetic oil improve tribological properties, ZnO in mineral oil exhibit excellent wear and friction reduction		0.5 wt%	[54]
CuO & Al_2O_3	PAO 8 & SAE 75W-85	< 50 nm	0.5, 1.0, 2.0 wt%	Homogenizer, 10 min & water bath, 3 h	Optimol SRV 4 reciprocating friction and wear tester	200 N	50 Hz	50 °C, 2 h	Reduce up to 14% (WSD) and 18% (COF) by addition of CuO in both base oil, while Al_2O_3 had a detrimental effect on both base oil		-	[59]
TiO_2	Water-based lubricant	20 nm	0.2–8.0 wt%	Ultrasonication with stirring, 10 min	Ball-on-disk tribometer	50 N	20 mm/s	Rt, 10 min	Can be decreased by 97.8%	Can be decreased by 49.5%	0.8 wt%	[56]
	Water-based lubricant	20 nm	0.4–8.0 wt%	Ultrasonication with stirring, 10 min	Ball-on-disk tribometer	5 N	50 mm/s	25 °C, 30 min	COF of oxidized disk is lower than clean disk, due to Fe element from steel ball oxidized and form a protective film		4.0 wt%	[55]
	Oil-in-water	30 nm	0.3–2 wt%	Stirring & ultrasonic vibration	Ball-on-disk tribometer	50 N	50 mm/s	80 °C, 30 min	Addition of 1 wt% oil + 2 wt% TiO_2 reduce 17.6% COF, other concentration are higher than base oil		1 wt% oil + 2 wt% TiO_2	[67]
CuO	Water based lubricant	20 nm	0.1, 0.2, 0.4, 0.6 & 0.8 vt%	Ultrasonic dispersed, 20 min	Four ball tribotester	147, 196 & 245 N	1440 rpm	Rt, 10 min	Addition of 0.2 wt% of CuO the friction reduce up to 69.2% and wear reduce up to 55.1% under different load		0.2, 0.4, 0.6 wt% at certain load	[68]

4.3. Metal Sulphides

Metal sulphides have been widely used for decades, as solid or liquid lubricant additives, including MoS_2, WS_2, FeS, CuS. It has been confirmed that nanoMoS$_2$ in liquid lubricants is better than microMoS$_2$ due to the smaller particles size for friction reduction [69]. MoS_2 as a lubricant additive in dioctyl sebacate results in more friction and wear reduction than microMoS$_2$ because of the extra formation of a solid and complex absorption film on the contact surface [70]. Fullerene-like NPs (IF) are the layered compounds with a hollow polyhedral structure. The addition of IF-MoS$_2$ and IF-WS$_2$ in PAO could significantly improve tribological properties [71]. Gulzar et al. [72] studied the tribological properties of chemical modified palm oil with the addition of MoS_2 and CuO, wherein nanoMoS$_2$ showed better tribological properties than nanoCuO. An interesting study discussed the anti-friction ability of nanoFeS with 20–200nm particle size as engine oil lubricant additive [73]. COF significantly decreases with the addition of nanoFeS and shows persistent anti-friction behavior under dry sliding. Figure 6 shows the formation of the sulfur diffusing area by the diffusion of S atom on the friction surface leading to friction reduction. The summary of metal sulphides as lubricant additives is shown in Table 4.
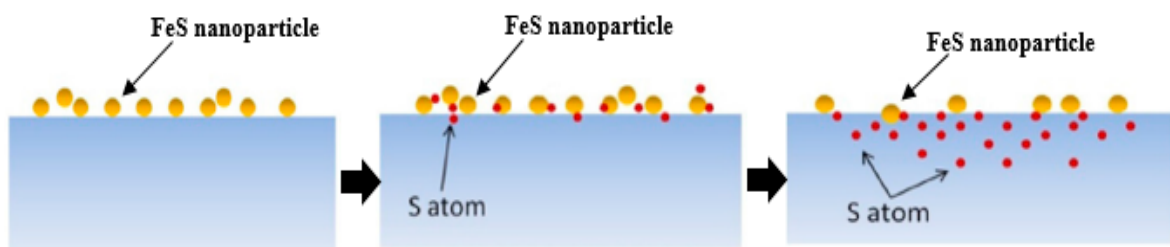

Figure 6. Diffusion of S-atom from FeS nanoparticles into the material surface [73].

Table 4. Summary of metal sulphides nanoparticles as lubricant additives.

Details of Nanolubricant				Dispersion Method, Duration & Temperature	Tribometer	Test Parameters			Test Results		Optimum Conc.	Ref.
Nanoparticle	Base Oil	Particle Size	Conc.			Load	Speed	Temp. & Duration	Wear Reduction	Friction Reduction		
Category: Mineral oil												
FeS	API SL/CF 10W-40 engine oil	20 -200 nm	0–2%	Mechanical stirring and ultrasonic dispersion	Pin-one-disc system	50 or 150 N	150 rpm	-, 20 min	Worn surface are more smoother and flatter	Decrease from 0.08 to 0.018 and 0.13 to 0.024 at different load	2 wt%	[73]
MoS_2	SE15W40	~50 nm	0.1, 0.5, 1.0, 2.0 & 5.0 wt%	High shear homogenizer, 30 min	Disc-on disc frictional testing machine	1500 N	500 rpm	Ambient temperature, 180 s	Enhance significantly the tribological performance of base oil		-	[74]
WS_2 nanorod 2H-WS_2	Mineral oil	10–15 nm	2 wt%	High speed dispersion machine, 20 min & ultrasonic bath, 30 min	Four ball tribotester	170, 245 & 320 N	1200 rpm	-, 30 min	Addition of WS_2 nanorod in oil show better tribological properties than base oil and 2H-WS_2		2 wt%	[75]
Category: Biolubricants												
MoS_2	Coconut oil & paraffin oil	90 nm	0.25, 0.5, 0.75, 1%	Ultrasonic shaker, 1 h, 50 °C	Pin-on-disc tribometer, four ball tester	2 to 4 MPA, 392 N	0.47 to 1.414 m/s, 600 rpm	-, 75 ± 2 °C, 60 min	Friction and wear reduce with the increase of concentration until reach optimum concentration		0.53% for coconut oil and 0.58% for paraffin oil	[76]
Category: Synthetic oil												
IF-MoS_2	Blend of PAO 4 & PAO 40	150 and 350 nm	1 wt%	Magnetic agitator	High frequency reciprocating rig (HFRR)	10 N	-	80 °C	All IF-MoS_2 were effective in friction and wear reduction, maximum friction reduced from 0.2 to 0.06		1 wt%	[69]
IF-MoS_2, IF-WS_2, 2H-MoS_2	PAO 6, PAO 40	50–80 nm	1 wt%	Ultrasonic bath	Ball-on-flat device, Pin-on-flat device	17.9 N, 2, 5 & 10 N	20 mm/s, 2.5 mm/s	25 °C	IF-MoS_2 exhibited the smallest wear rate and COF as low as 0.03		1 wt%	[71]
Multi-wall nanotubes MoS_2	PAO	100–500 nm	5 wt%	Ultra-sound, 1 h	Ball-on-disc tester	10 N	0.005 m/s	Rt	Reduced between 5–9 times	Reduced by more than 2 times	5 wt%	[77]
IF-MoS_2, IF-WS_2, Re:IF-MoS_2, 2H-MoS_2	PAO-6	100 nm, 120 nm, 100 nm, ≤2 μm	-	Mechanical stirrer IKA T25 Ultra-Turrax disperser, 30 min	Rotational disc Tribometer	30, 60 90 N	2.1 m/s	25, 50 & 80 °C, 16 min	IF nanoparticles exhibited enhance tribological performance as compare to 2H-MoS_2, and reduction of 40% COF		-	[78]
Category: Others												
MoS_2	Dioctyl sebacate	50–100 nm	0.25, 0.5, 1.0, 1.5, 2.0 wt%	Ultrasonic oscillation, 30 min	High frequency reciprocating ball-on-disc tribometer	7.84 N	0.1 m/s	60 °C, 75 min	Reduced by ~35%	Reduced by ~37%	-	[70]

4.4. Carbon-Based Nanoparticles

From here use of carbon-based NPs as lubricant additives is still an innovation. These include diamond, graphene, and graphite. Peng et al. reported that diamond NPs in paraffin oil exhibit excellent tribological properties due to the formation of a protective film, which separates the friction surface [79]. It should be noted that changes of adhesion to abrasion wear mechanism improve the tribological behavior of PAO with an optimum concentration of 0.2 wt% diamond NPs [80].

The lubrication mechanism of graphite NPs can be the mending effect, the formation of tribofilm, and rolling effect. Gupta et al. [81] reported the highest tribological performance of improvement up to 80% by graphite with dispersant. The enhancement of AW properties is related to the combination of formation of tribofilm and mending effect, and the tribofilm formation mechanism contributes to EP enhancement. Sivakumar et al. [82] reported graphite oxide as the lubricant additives which are synthesized by the waste carbon sources, that reduce friction wear and surface roughness by up to 21.1%, 18.5%, and 42.3%, respectively.

Graphene is highlighted out of all the NPs due to its unique properties, including excellent mechanical, physical, and electrical properties. Further, graphene has been used in various applications, and is frequently named a "supermaterial" or "all-in-one material" in the world of material science [83]. The improvement of friction and wear is up to 80% and 33% with the addition of graphene in engine oil and the enhancement is related to the ball-bearing effect and ultimate strength properties of graphene [84]. A comparative study between modified natural flake graphite and modified graphene platelets in SN350 base oil has been conducted by Lin et al. The results showed that modified graphene platelets have better tribological properties [85]. Graphene by exfoliation should also be mentioned [86,87]. The ocradecylamine reduced graphene oxide nanolubricants in boundary regime and hydrodynamics regime has been evaluated by Vats et al. The results showed that the COF reduced by 61.8% and 75% in those regimes and WSD significantly decreased by 92.5% in the boundary regime [88]. Besides, the viscosity of these nanolubricants improved by 60% through flow analysis. The summary of carbon-based NPs as lubricant additives is shown in Table 5.

Table 5. Summary of carbon-based nanoparticles as lubricant additives.

Nanoparticle	Base Oil	Particle Size	Conc.	Dispersion Method, Duration & Temperature	Tribometer	Load	Speed	Temp. & Duration	Wear Reduction	Friction Reduction	Optimum Conc.	Ref.
Details of Nanolubricant						Test Parameters			Test Results			
Category: Mineral oil												
Diamond	Paraffin oil	110 nm	0.025–5 wt%	Ultrasounds, 30 min	Ball-on-ring tester	50–300 N	500 rpm	Rt, 60 min	Maximum reduction of wear up to ~23.73%	Maximum reduction of COF up to ~14.77%	0.2 wt%	[79]
	CPC R68 commercial oil	4.37 ± 0.45 nm	1, 2, 3 vol%	Stirring, 1 h, 60 °C & supersonic redispersed	Blocks-on-ring configuration	-	4.87, 6.084, 7.30 m/s	-	Nano-diamond improve anti-scuffing performance and addition of 2/3 vol% result large friction reduction		-	[89]
Graphite	API Group III 150 N base oil	55 nm	1–4 wt%	Ultrasonic probe, 35 min	Four ball tester	392, 588 & 784 N	1200 rpm	75 °C, 1 h	Highest performance improvement up to 80% by graphite with dispersant		3 wt%	[81]
Graphene	Engine oil	-	0.0125–0.06 mg/mL	Probe sonicator, 60 min	Four ball tester	392 N	600 rpm	75 °C, 60 min	Improve up 33%	Improve up to 80%	0.025 mg/mL	[84]
Modified natural flake graphite (MNFG) & modified graphene platelets (MGP)	SN350 base oil	25 μm	0.015–0.105 wt%	Magnetic stirrer, 1 h, 80 °C	Four ball machine	147 N	1200 rpm	75 ± 2 °C, 60 min	COF of MGP-based oil was lower than base oil and MNFG-based oil, overall lubricious properties of lubricating oil had improved with the addition of MGP		0.075 wt%	[85]
Graphene (liquid phase exfoliation)	SAE10W-30	3–5 μm	0.025, 0.05, 0.075 & 0.1 wt%	Stirring, 120 min	Pin-on-disk tribometer	125.66 N	191 rpm	25 ± 1 °C, 7200 s	Addition of graphene in SAE 10W-30 decrease wear rate and reduces COF		0.05 wt%	[87]
Octadecylamine reduced graphene oxide (ODA-rGO)	Liquid paraffin oil	500 nm	0.2 wt%	Ultrasonic bath, 120 min	Four ball tester (boundary lubrication regime), ball-on disc tribometer (EHL regime)	392 N,20 N	1200 rpm, 1–2000 mm/s	60 min, -	Significantly reduced by 92.5%	Reduce by 61.8% in boundary regime and 75% in EHL	0.2 wt%	[88]
Category: Synthetic oil												
Diamond	PAO	60–90 nm	0.2, 0.4, 0.6 & 0.8 wt%	Ultrasonic probe, 30 min	Ball-on-disc	100 N	0.58 m/s	-	Concentration increase, result in more wear and friction		0.2 wt%	[80]
Graphite	PAO 4	10–50 nm	0.01 wt%	Stirring, 10 min & ultrasonic vibration, 15 min	Ball-plate contact wear testing machine	10 N	5 mm/s	25 ± 2 °C, 100 °C & 175 °C, 6000 s	Wear rate reduce at least 90% with addition of graphite at 175 °C	From 0.2 decrease to 0.12 at Rt & from 0.55 decrease to ~0.16 at 100 °C	0.01 wt%	[90]
Graphene—different degree exfoliation	PAO 6	1~2 μm	0.1, 0.5, 1.0, 2.0 wt%	Magnetic stirrer, 3 h & ultrasonication, 0.5 h	Reciprocating sliding tester	2 N	-	-	Few layer graphene (FLG) with larger interlayer spacing exhibit lower friction		0.5 wt% for FLG-Ms- based oil	[86]
Graphene	PAO 9	-	0.01–5 wt%	Ultrasonication, 15 min	Four ball tribometer	400 N	1450 rpm	Rt	Reduced by 14%	Reduced by 17%	0.02–0.06 wt%	[91]
Category: Biolubricants												
Graphite	LB2000 vegetable based oil	35&80 nm	0.05–0.25 vol%	Ultrasonic cleaner, 1–1.5 h, 25 °C	Pin-on-disk friction and wear tester	2, 10 N	100 rpm	24 °C	The increase the volume fraction of nano-graphite, the lesser the COF and wear		0.25 vol%	[92]
Graphene	Palm oil based vegetable oil	-	25, 50, 100 ppm	Ultrasonicator, 1 h	Four ball tribotester	392 N	1200 rpm	75 °C, 1 h	Wear and friction decrease with the addition of 25 & 50 ppm graphene		50 ppm	[93]
Category: Others/Mixed test oil												
Graphene	SAE20W40 + Modified jojoba oil	-	0.05, 0.075, 0.1 wt%	Magnetic stirrer, 120 min	Pin-on-disc setup	50, 100, 150 N	1–5 m/s	-	JO20 (80 vol% of SAE20W40 + 20 vol% of modified jojoba oil) with the addition of 0.075 wt% result in the lowest wear and friction		0.075 wt%	[94]
	Hydraulic oil	2 μm	1 wt%	Magnetic stirrer, 30 min & Ultrasonic mixing, 1 h, 50 °C	Ball-on disk	3 N	1.2–38.4 mm/s	25~125 °C	Multilayer graphene as additive results relatively high and unstable tribological properties		1 wt%	[95]

4.5. Nanocomposites

These are multicomponent materials, including WC-Al$_2$O$_3$/graphene platelets, Cu/graphene oxide, TiO$_2$/SiO$_2$, Ag/graphene, graphite oxide/Cu, and Al$_2$O$_3$/TiO$_2$, etc. Due to the synergistic effect of the combination of NPs, nanocomposites usually provide better performance than single NPs. One should note that the nanocomposites which include graphene exhibit excellent tribological performance [14,96–98]. The tribological properties of WC-Al$_2$O$_3$/graphene platelets has been investigated. The test under 40 and 60N load show that the COF incorporated with graphene is 40.4% and 33.3% lower than test carried out without graphene. Further, the addition of graphene changes from significant abrasive wear to minor abrasive wear [99].

It is of interest to study tribological properties of TiO$_2$/SiO$_2$ NPs in palm TMP ester, even without the use of surfactant, because the dispersion stability is stable and also effective in friction and wear reduction. At the same time, the surface is enhanced by the mending and polishing effect [100].

Composites of Cu-MoS$_2$ and Ag-MoS$_2$ reduce the COF and essentially improve wear resistance [101]. Copper/carbon nanotube nanocomposite results in a reduction of friction and wears by up to 23.7% and 33.5%, respectively [102]. Both studies report that the improvement of lubrication is related to the synergistic effect of nanocomposites. Various studies of nanocomposites as lubricant additives are shown in Table 6.

Table 6. Summary of nanocomposites as lubricant additives.

Details of Nanolubricant				Dispersion Method, Duration & Temperature	Tribometer	Test Parameters			Test Results		Optimum Conc.	Ref.
Nanoparticle	Base Oil	Particle Size	Conc.			Load	Speed	Temp. & Duration	Wear Reduction	Friction Reduction		
Category: Mineral oil												
Ag/graphene nanocomposite (with laser irradiation)	Paraffin oil	56 nm	0.05, 0.1, 0.15 & 0.2 wt%	Ultrasonication, 30 min	Four ball tribometer	392 N	1200 rpm	Rt, 30 min	Reduction up to 36.4%	Reduction up to 40%	0.1 wt%	[97]
Nano-Cu/graphene oxide composite	Paraffin oil	5–10 nm	0.05 wt%	Ultrasonication, 30 min	Four ball tribometer	200 N	1200 rpm	Rt	Reduced by 52.7%	Reduced by 27%	0.05 wt%	[14]
Sc-Ag/GN (Silver decorated graphene)	10w40 engine oil	3–9 nm	0.6~0.1 wt%	Ultrasonication, 30 min	Four ball machine	343 N	1200 rpm	75 ± 1 °C, 1 h	Reduced up to 27.4%	Reduced up to 30.4%	-	[103]
Nano-Ag/MWCNTs	10w40 engine oil	5–15 nm	0.03–0.27 wt%	Ultrasonically dispersed	Four ball machine	392 N	1200 rpm	75 ± 1 °C, 1 h,	Reduced up to 32.4%	Reduced up to 36.4%	0.18 wt%	[104]
Al_2O_3/TiO_2	5W-30 engine oil	8–12 nm	0.05, 0.1, 0.25 & 0.5 wt%	Magnetic stirrer, 4 h	Piston ring/cylinder liner tribometer	40–230 N	0.5–1.45 m/s	100 °C, 20 min	Decrease up to 17%	Decrease up to 47.61%	0.1 wt%	[105]
Category: Biolubricants												
Nano-TiO_2/SiO_2	Palm TMP ester	37 nm	0.25, 0.5, 0.75 & 1 wt%	Ultrasonic probe, 30 min	Four ball extreme pressure & piston ring-cylinder liner sliding tribotester	40 kg, 160 N	1770 ± 30 rpm, 500 rpm	25 ± 5 °C, 10 s, 70 °C, 2–6 h	Reduce as much as 10.4%	Reduce as much as ~16.12%	0.75 wt%	[100]
Copper/carbon nanotube nanocomposite	Rapeseed oil	4–7 nm	0.05, 0.1, 0.2, 0.3 & 0.5 wt%	Ultrasonication, 1 h	Ball-on-disk apparatus	1–12 N	100–500 rpm	30 min	Reduction up to 23.7%	Reduction up to 33.5%	0.2 wt%	[102]
Category: Others/none												
Graphene oxide/copper nanocomposite	polyethylene glycol (PEG 200)	15–20 nm	0.02, 0.04, 0.06, 0.08 & 0.1 wt%	Ultrasonication, 60 min	Multifunction sliding friction tester & four ball friction device	1–8 N & 392 N	2 Hz & 1200 rpm	60 min	Improve wear resistance up 47%	Improve friction resistance up 40.1%	0.08 wt%	[98]
WC- Al_2O_3 with graphene platelets (GPLs)	-	<2 μm	0.3 wt% GPLs	-	Reciprocating tribometer	40 & 60 N	350 rpm	25 °C, 150 min	The specific wear rate are one order of magnitude lower than without addition of GPLs, the COF reduce up to 40.4%		0.3 wt%	[99]
Cu-MoS_2 & Ag-MoS_2	Litol and VNIINP greases	-	2–50 wt%	Ultrasonic bath	Ball-on-disk tribometer	5 N	5 cm/s	30 min	Cu-MoS_2 and Ag-MoS_2 reduced the COF and essentially improve wear resistance		-	[106]
(Zn-Ni)/Al_2O_3	-	30 nm	-	Ultrasonication with magnetic stirrer, 120 min, 30 °C	Pin-on-disk method	10 N	10 mm/s	Rt	Weight loss from 4.6 mg to 3 mg	From 0.578 to 0.392	-	[107]
Hybrid Cu-Al_2O_3/Graphene platelets	-	<100 nm	0.3, 0.6, 0.9, 1.2 wt%	Planetary ball mill, 2 h	Pin-on-disc tribometer	5, 10, 15 & 20 N	0.4, 0.7, 1 m/s	-	The wear resistance increase and COF is decrease by increasing the concentration of graphene platelets		1.2 wt%	[108]

4.6. Rare Earth Compounds

Rare earth compounds can be used as lubricating additives or doped to other NPs. Typically, the lubrication mechanism of rare earth compounds is the formation of a tribofilm or absorption film. La-doped Mg/Al layered double hydroxide NPs modified by sodium dodecyl sulfate show better friction properties than those without modification in diesel engine oil CD 15W–40. The lubrication mechanism has been concluded as the formation of tribofilm on the friction surface leading to friction reduction [108]. Cerium oxide provides excellent tribological properties even in titanium complex grease or lithium grease [109,110]. Furthermore, the tribological properties of rare earth compounds such as LaF_3 and $CeVO_4$ have also been investigated [111,112]. Few examples of rare earth compounds as lubricant additives are shown in Table 7.

Table 7. Summary of rare earth compounds as lubricant additives.

Details of Nanolubricant				Dispersion Method, Duration & Temperature	Tribometer	Test Parameters			Test Results		Optimum Conc.	Ref.
Nanoparticle	Base Oil	Particle Size	Conc.			Load	Speed	Temp. & Duration	Wear Reduction	Friction Reduction		
Category: Mineral oil												
Layered double hydroxide (LDH)-La-doped Mg/Al	Diesel engine oil (CD 15W-40)	185.96 nm	0.5 g LDH per 100 mL oil	Ultrasonic bath, 80 °C	Four ball tester	392 N	1200 rpm	Rt, 60 min	Reduced by 12.9%	Reduce from 0.111 to 0.093	-	[103]
CeVO$_4$ (Cerium orthovanadate)	Liquid paraffin oil	30–50 nm	0.2, 0.4, 0.6 & 0.8 wt%	-	Seta shell four ball machine	300 N	1459 rpm	30 min	Result show addition of CeVO$_4$ exhibited good anti-wear		0.6 wt%	[107]
Category: Others												
CeO$_2$	Titanium complex grease	<10 nm	2 wt%	-	Four ball machine	392 N	1450 rpm	25 °C, 10 s; 75 °C, 60 min	Tribological properties were significantly improved		2 wt%	[105]
	Lithium grease	<500 nm	0.2, 0.4, 0.6, 0.8 & 1.0 wt%	Ultrasonic dispersion instrument, 20 min	Four ball friction and wear testing machine	392 N	1200 rpm	75 °C, 60 min	Decrease up to 13%	Decrease up to 28%	0.6 wt%	[104]
LaF$_3$	Fluoro silicone oil	10–30 nm	0.02, 0.04, 0.06, 0.08 & 1.0 wt%	-	Four ball friction and wear tester	300 N	1450 rpm	25 °C, 30 min	The friction and wear decrease, until the concentration reach 1.0 wt%		0.08 wt%	[106]

5. Lubrication Mechanism of Nanoparticles

From here nanoparticles as the lubricating additives in lubricants are applicable to reduce the friction and wear and increase the load capacity of mechanical parts. Studies of lubrication mechanisms will serve as a decisive parameter to understand the tribological properties of nanolubricants. The lubrication mechanism of nanoparticles already purposed includes the ball bearing effect, protective film formation, mending effect, and polishing effect. These mechanisms are mainly classified into two groups. The first group is the direct action of NPs in lubrication enhancement (ball bearing effect/protective film formation) and the second group is surface enhancement (polishing/mending) [113].

5.1. Rolling Effect

Additionally known as the ball-bearing effect, normally the spherical or quasi-spherical nanoparticles act as ball bearings that roll between the contact surface and convert sliding friction to the combination of sliding and rolling friction [79], as shown in Figure 7. Various studies examining the ball-bearing mechanism have been carried out. Viesca et al. [48] evaluated carbon-coated copper nanoparticles and stated that tribological improvement is related to the ball-bearing mechanism. Wu et al. [55] investigated the tribology properties of TiO_2 nanolubricants by ball-on-disk tribometer. They reported this type of nanolubricants evidenced the ball-bearing effect between ball and disk with a demonstration from SEM micrograph as shown in Figure 11a. Raina and Anand [80] demonstrated the nearly spherical shapes of diamond nanoparticles ability to reduce the sliding contact surface, and this is associated with the ball bearing mechanism.
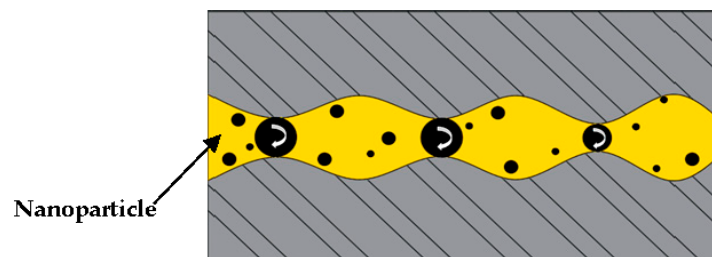
Figure 7. Rolling mechanism by NPs-based lubricant [22].

5.2. Protective Film Formation

Nanoparticles are more likely to form an amorphous layer (protective film) on the friction surfaces in this mechanism [79], as shown in Figure 8. Tribo-film is the protective film on material surfaces. Tribo-film and near-surface materials decide the tribological behavior of the contacting surface. The reaction between substrate and nanoparticles form the film under the environment condition or tribo-sintering [114]. Several experimental studies have reported the mechanism of tribo-film formation to provide excellent lubrication. Meng et al. [108] reported that silver decorated graphene nanocomposite forms a protective film that smoothens and reduces the surface roughness of the contact area. Protective film formation has an energetic effect on the life of friction parts reported by Wang et al. [115]. Zhao et al. [86] demonstrated that the protective tribofilm formed by graphene indeed attains slippage between friction surfaces, therefore leading to better lubrication, as shown by the SEM and HRTEM micrograph of protective film formation in Figure 9. Some studies reported wear reduction [64,116], wear and friction reduction [112] via the protective film formation mechanism. Liu et al. [117] determined the strength and ductility of the protective film. They report that strength is necessary under low frequency while ductility important under high frequency. The formation of a protective film can be demonstrated using analysis techniques such as scanning electron

microscopy/energy dispersive X-ray spectroscopy (SEM/EDS), X-ray photoelectron spectroscopy (XPS), and Raman spectroscopy.
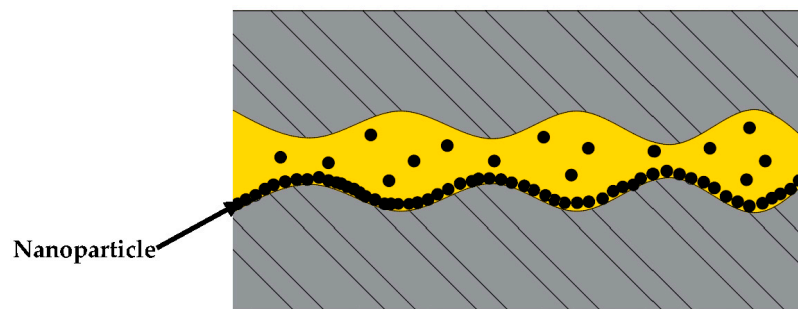

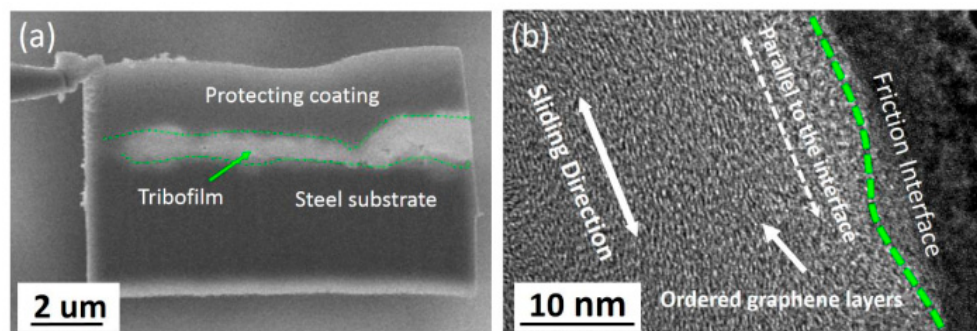**Figure 8.** Protective film formation mechanism by NPs-based lubricant [22].

Figure 9. (**a**) SEM micrograph of tribofilm formation on steel substrate; (**b**) HRTEM micrograph of tribofilm formation beside the friction interface [86].

5.3. Mending Effect

The mending or self-repairing effect characterized by nanoparticles deposition on the rubbing surfaces compensates mass losses [79], as shown in Figure 10. In addition, nanoparticles are also deposited on the wear surface and fill the grooves during this mechanism. Yadgarov et al. [78] report that low friction and wear scar is because of the mending effect, and IF-nanoparticles also contribute to this. The self-repair effect has been reported by using graphene/Ag nanocomposite [97]. SEM/EDS analysis can be used to verify the mending effect on the rubbing surface. Figure 11b shows the direct evidence to support this lubrication mechanism on the rubbing surface.
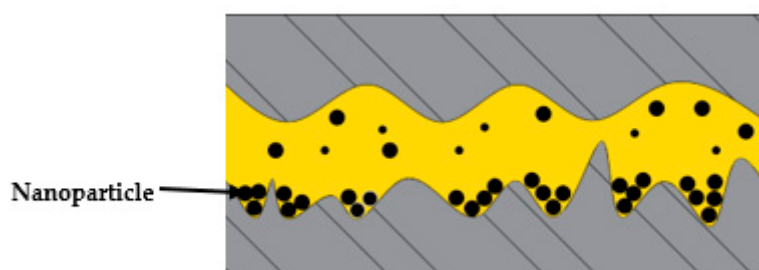
Figure 10. Mending effect mechanism by NPs-based lubricant [22].
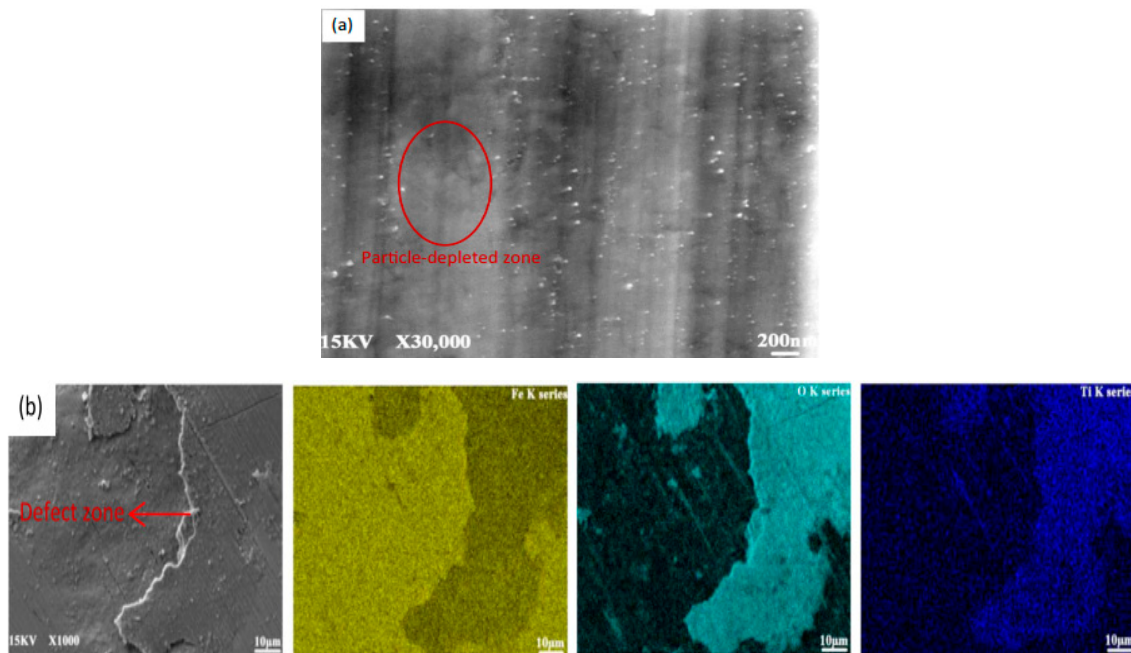
Figure 11. (**a**) The demonstration from the SEM micrograph for rolling effect; (**b**) the mending effect on the rubbing surface analyzed through the SEM/EDS analysis [56].

5.4. Polishing Effect

The polishing effect also called the smoothing effect, reduces the lubricating surface roughness by nanoparticle assisted abrasion [113], as shown in Figure 12. Ignole et al. [60] reported that TiO_2 nanoparticles consisting of anatase and rutile phase had a more polishing effect on the surface. Wu et al. [56] also reported that TiO_2 nanoparticles filled the defects found on the friction surfaces. One of the mechanisms mentioned by Koshy et al. for the surface roughness reduction is that the nanoparticle fills the asperities [76]. They measured the surface roughness of the friction surface by atomic force microscopy (AFM) and the AFM images (before and after sliding) show the reduction of surface roughness, as shown in Figure 13. In addition, the SEM micrograph provides evidence of the polishing effect with the presence of Al_2O_3/TiO_2 nanocomposites, as shown in Figure 14.
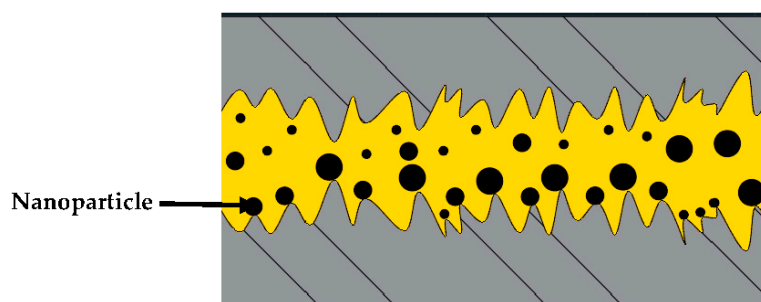
Figure 12. Polishing effect mechanism by NPs-based lubricant [22].
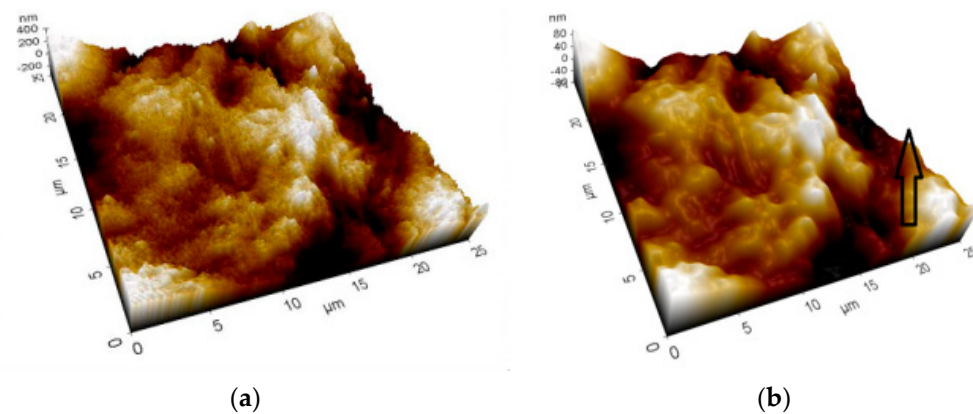
Figure 13. (**a**) AFM images of friction surface before sliding (surface roughness = 143 nm); (**b**) AFM images of friction surface after sliding (surface roughness = 68 nm) [76].
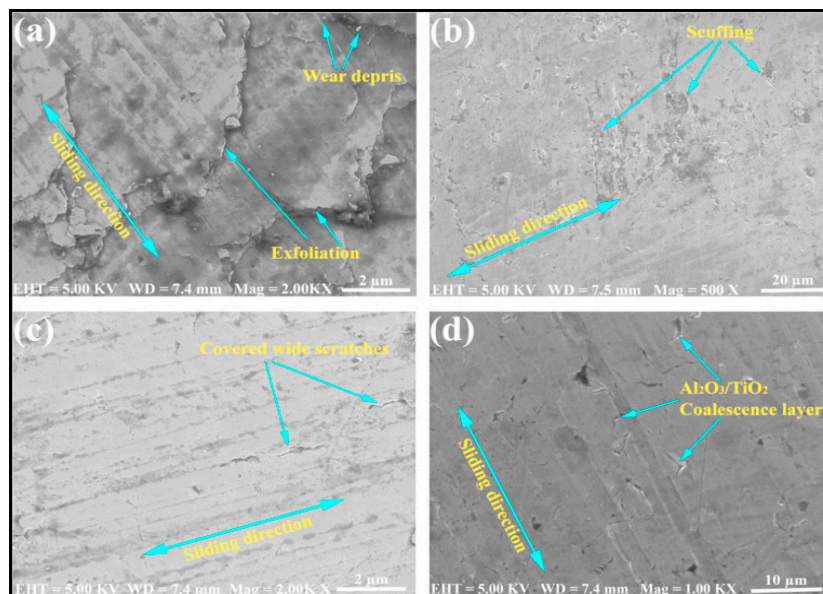

Figure 14. (**a**,**b**) SEM micrograph of the worn surface with commercial lubricant; (**c**,**d**) SEM micrograph of the worn surface with Al_2O_3/TiO_2 nanolubricants [110].

6. Parameters of Nanoparticle Affect the Tribological Properties

6.1. Concentration of Nanoparticles

Concentration is one of the most critical factors that affect the tribology characteristics of nanolubricants. In most cases, the addition of NPs in the lubricant is useful in reducing friction and wear. There is also no ideal concentration, even with the addition of below 1 wt% concentration NPs [94] or above 2 wt% concentration NPs [55], but adding more NPs in the lubricant does not mean any concomitant increased reduction in friction and wear. Still, there is an optimum concentration for maximum reduction of friction and wear. Rajubhai et al. [49] investigated tribological characteristics of copper NPs in Pongamia oil with different concentrations of 0.025, 0.05, 0.075, and 0.1 wt% with the results revealing that 0.075 wt.% is the optimum concentration with minimum evidence of friction and wear. Shaari et al. [65] reported that an addition of 0.1 wt.% TiO_2 in palm oil exhibits the lowest friction and wear. Stephen et al. [93] investigated the tribological effect of graphene in palm oil with the addition of 25, 50, and 100 ppm and reported that 50 ppm is the optimum concentration. Zhang et al. [52] added Sn and Fe in macs base oil with concentrations of 0.1, 0.5, and 1.0 wt%, with the results showing that optimum concentration of both nanoparticles is 1.0 wt%, although Sn was more effective in friction

reduction and Fe more effective in wear reduction. The addition of MoS_2 in coconut oil and paraffin oil was investigated by Koshy et al. [76]. The optimum concentration of MoS_2 obtained from these base oils is slightly different. The optimum concentration of coconut oil is 0.53 wt%. In comparison, paraffin oil is 0.58 wt%. This investigation can show that the optimum concentration of nanoparticle is related to the base oil too. Furthermore, Alves et al. [54] added an optimum concentration of 0.5 wt% nanoCuO and nanoZnO to investigate tribological properties in mineral oil, PAO, sunflower oil, and soybean oil, but this research contains a contradiction on their experiment results. Azman et al. [66] added an optimum concentration of 0.34 wt% nanoCuO in palm kernel oil. The results show that friction and wear is reduced by 56% and 48%, respectively.

6.2. Size of Nanoparticles

NP size is an important parameter that directly affects the tribological performance of nanolubricants. The smaller the particle size, the easier it is to penetrate the rubbing surface. The reaction is dependent on the surface-to-volume ratio and the particle size determines the hardness of NPs, which conversely affects the tribological properties [114]. For nanomaterials with a size range of 100 nm or higher, a decrease in particle size corresponds with an increase in the hardness. This is due to the Hall–Petch regime. In contrast, for particle sizes usually below 10nm, a decrease in particle size corresponds with the softer nanomaterials. This explanation is called the inverse Hall–Petch regime. If the hardness of NPs is higher than the hardness of tribo-pair materials, this will result in indentation and scratches [6]. Peña-Parás et al. [59] reported that 8-9 Mohs hardness of nanoAl$_2$O$_3$ higher than the metal substrate causes the NPs in base oil re-agglomeration and abrasion. Thus, the size and hardness of NPs should be considered in the preparation of nanolubricants.

Furthermore, the ratio of root mean square (RMS) roughness of the lubricated material surface to the NPs radius is essential in selecting suitable NPs size. Nanolubricants must keep providing the lubrication on the contact zone during operation to protect the material surface. For this reason, if the NP size is larger than the gap between asperities, the NPs could not fill in the contact zone, potentially leading to inadequate lubrication.

To obtain stable nanolubricants, the NPs must homogeneously disperse in the base oil. Therefore, the dispersion stability is a function of NP size, which is considered a crucial factor in the preparation of nanolubricants. The dispersion stability can be determined by the sedimentation rate and calculated by using Stokes' law:

$$V_z = \frac{2(\rho_{NP} - \rho_F)gr^2}{9\mu}$$

where, v_z is settling velocity, ρ_{NP} is the mass density of NPs, ρ_F the is mass density of fluid, g is gravity, r is the radius of NPs, and μ is dynamic viscosity.

Based on the Stokes' law, smaller particle size indicates better dispersion stability and results in achieving stable nanolubricants. Chen et al. [47] evaluated the tribological properties of Ni-based nanolubricants with 7.5, 13.5, and 27.5 nm of diameter. They reported that Ni-based nanolubricants with 7.5 nm diameter exhibited effective anti-wear ability compared to another two. The investigation by Su et al. [92] demonstrated that graphite-based nanolubricants with smaller particle sizes are more effective in improving tribological performance at the same volume fraction.

6.3. Morphology of Nanoparticles

The shape of NPs is vital in the preparation of nanolubricants, because it is relevant to the pressure experienced by NPs through loading. NPs have five types of form: spherical, granular, onion, sheet, and tube. Most NPs are in the spherical shape, followed by granular, sheet, onion, and tube. After nucleation, to achieve equilibrium, the particle crystalline structures tend to change, and the surface energy will be minimized. NPs form in spherical shape if there is isotropic surface energy [38]. Normally, spherical shape NPs favor the rolling mechanism, it will act as ball-bearing roll between the friction surfaces. Mostly spherical shaped nanoAl$_2$O$_3$ act as ball bearing and lead to improving load

capacity, friction, and wear reduction [58] and nearly spherical shaped nanoCu show improvement in tribological properties from SEM and EDS analysis [48]. In addition, the relationship between the shape of NPs contact to the lubricated surface are important too. Spherical shaped NPs result in point contact with surface(s) through loading. The line contact is related to nanosheets, yet nanoplatelets are planar contact [114]. The schematic diagram demonstrating the effect of nanoparticle shape upon loading is shown in Figure 15.
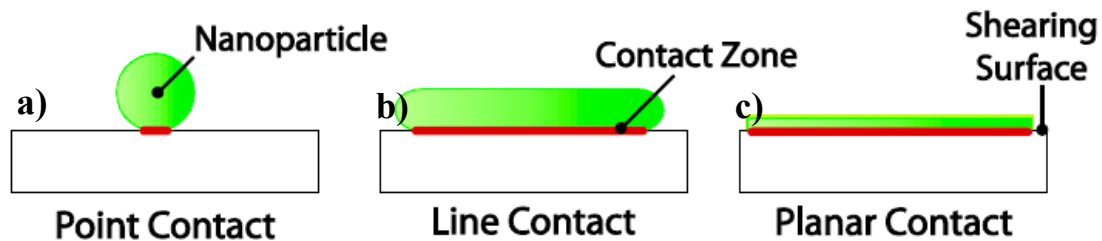
Figure 15. Schematic diagram of the effect of nanoparticle shape upon loading: (**a**) point contact, (**b**) line contact, (**c**) planar contact [118].

Onion morphology has an external spherical shape and internal lamellar structure. Stability of the onion morphology corresponds to the tribological performance. If it is stable, it will be similar to the spherical morphology, or else it becomes sheet morphology by exfoliating. The advantage of onion-shaped NPs is a lack of dangling bonds [38]. The presence of dangling bonds generates high local energy, which could affect some physical properties of NPs. Therefore the reaction of NPs with the environment is easier or reduces the energy by agglomeration [119]. Since dangling bonds are absent in onion morphology, the reaction between particles and environment will be weakened, which results in less particles attaching to the substrate. The sheet-like NPs consist of graphene, ZrP, hBN, and transition metal dichalcogenides. Lubrication in this case is about the exfoliation between adjacent layers by sliding and leading to friction reduction.

Furthermore, in addition to NP morphology affecting tribological properties, the internal nanostructure is also a factor. The tribological properties of WS_2 nanorod as nanoadditives in mineral oil has been investigated [75]. They also compared the tribological properties of WS_2 nanorod with 2H-WS_2 (mix layer). WS_2 nanorod lubricant shows better tribological properties with the formation of a thin tribofilm on the substrate, followed by 2H-WS_2 and base oil. Tribological performances had been improved by liquid-phase exfoliation graphene as an additive in SAE 10W-30 oil. Another study explained the layered structure of transition metal dichalcogenides in friction reduction with the formation of tribofilm [120]. Compared to the typical transition metal dichalcogenides, IF-NPs consist of layered compounds with a hollow polyhedral structure. Hence, this results in excellent lubrication with three lubrication mechanisms: rolling, sliding, and exfoliation [121]. The significant improvement of tribological performance of the metallic substrates is with the addition of IF-MoS_2 [71]. Rabaso et al. [69] reported the benefits of using IF-MoS_2 including size and morphology, which does not affect the tribological performance, and is more effective than bulk h-MoS_2. In investigating how to obtain further improvement in the tribological performance of IF-NPs, Yadgarov et al. [78] doped the IF-MoS_2 with rhenium and reported that it obtained a better result than IF-MoS_2.

6.4. Dispersion Stability of Nanoparticles

The high surface area to volume ratio in NPs leads to high surface energy. High surface area means the molecular attraction is strong and causes the particles to agglomerate. The aggregation of NPs results in sedimentation and also a loss of tribological improvement ability. Thus, the dispersion stability of NPs is strongly desirable for reliable lubrication performance. Stability is defined as the NPs not agglomerating at a significant rate. Several methods can enhance dispersion stability. The currently proposed methods are ultrasonic agitation, high-shear mixing, homogenizing, ball milling,

and magnetic force agitation [122]. Various studies have mentioned the method that they used for dispersion including magnetic stirrer [42,60], ultrasonic probe agitation [84], homogenization by triple-roller mill [51] and planetary ball mill [112], ultrasonic bath agitation [65], ultrasonic shaker agitation [57,61], high shear homogenizer [74], and mix method [46,73,86]. According to the literature, the majority of researchers use ultrasonic agitation for NPs dispersion, even though some of them just mentioned ultrasonication for dispersion or failed to mention any method at all. Zhao et al. [86] reported that graphene disperses in base oil with similar dispersion stability leading to eliminating the factor that affects lubrication properties. Furthermore, dispersion duration is also an important parameter to reduce or control agglomerations. It has been concluded that with the increase of mixing time, the size of NPs aggregates decreases by using magnetic force agitation [123]. The dispersion duration was carried out by the researchers as short as 5 min [52], and as long as 8 h [64], while the majority dispersion duration is 30 min or 1 h.

In addition, it is not only the dispersion methods that can reduce the agglomeration of NPs. The surface functionalization has developed to enhance dispersion stability. These include electrostatic stabilization and steric stabilization. Electrostatic stabilization is when the ionic surfactants have been absorbed on the NPs surface, while steric stabilization is achieved by applying a polymer or surfactant coat on the NPs surface. The surface-functionalized NPs should have better lubrication compared to bare NPs. The former prevents material transfer that leads to avoiding direct contact and cold-welding between shearing surfaces. Additionally, a rigid internal core and soft external shell in the hybrid structure of functionalized NPs allows for high load carrying capacity and does not reduce the lubrication [6]. Hence, surface-functionalized NPs provide more benefit compared to bare NPs.

The surface functionalization technique and related studies will be discussed. Surface modification is one of the methods to enhance dispersion stability. The common modification agent such as oleic acid is widely used in various studies to enhance dispersion stability [44,63,85]. In addition, other modification agents have been studied. NanoCu has been surface modified using a mixture of resin, methylbenzene, and amine compound, and the prevention of agglomeration and good oil-dispersion ability has been confirmed [8]. NanoCu surface modification by methyl-methyl acrylate provides a benefit in reducing friction and wear [50]. The surface-modified nanoPd by tetrabutylammonium chains results in the extension of loading parts life and electrical conduction [53,124]. One should note that dual modified CuO by sodium oleate (SOA) and alkylphenol polyoxyethylene ether disperse in water, resulting in excellent dispersion stability and improvement in lubricity [68]. Another noted study showed that the surface-capped triangle Cu nanoplates prepared by cetyltrimethylammonium bromide (CTAB) were effective in wear loss reduction (82%) and friction reduction (12%) by the formation of tribofilm at the interface of the parts [51].

Furthermore, the second method is to use a surfactant to enhance dispersion stability. Surfactants can also be considered as a dispersant, and using this method is easier and more economical than the surface modification method because the surfactant can be directly added in nanolubricants. Still, the cons of using surfactants have a limitation on thermal conductivity enhancement. Used surfactants include oleic acid [46,62,72,91], sodium-dodecyl [103], sorbitol monooleate (SPAN 80) [74,75,90], and polyisobutylene succinimide (PIBSI) [81]. Demas et al. [125] studied the dispersion stability of nanoBN and nanoMoS$_2$ by using five types of surfactant. They proved that using a surfactant not only benefits in suspending the NPs, but also decreases friction and wear by itself. Four types of dispersant have been selected to explore the dispersion stability and influence of EP properties in API Group III 150N base oil with or without hBN particles [126]. All dispersants impart their dispersion stability and influenced tribological properties of oil. One should note that 1% dispersant did not influence EP properties of oil, and 5% dispersant shows more improvement of dispersion stability along with a 10% EP performance increase. The EP performance increased by up to 30% by adding the hBN particle.

Methods to Analyze Dispersion Stability of Nanolubricants

There are a number of ways to evaluate the dispersion stability of nanolubricants. These include the sedimentation method, zeta potential analysis, spectral absorbency analysis, and metallographic micrograph stability test [114]. In addition, the centrifugal method has also been mentioned [68]. Table 8 provides a summary of the evaluation of dispersion stability of nanolubricants.

Table 8. Summary of evaluation on dispersion stability.

Nanoparticle	Lubricant	Method	Surface Modified/Dispersant	Result	Ref
Graphite	API Group III 150 N base oil	Sedimentation	1 wt% Polyisobutylene succinimide (PIBSI)	Without dispersant sediment after 6 days, while with dispersant the stability up to 50 days	[81]
Graphite	PAO 4	Sedimentation	1 wt% Sorbitan monooleate (span 80)	The precipitation occurs after 72 h which including dispersant	[90]
CuO	Palm kernel oil (PKO)	Sedimentation	-	Fully precipitated after 16 days	[66]
	Water based lubricant	Sedimentation, Centrifugal method	Coated by sodium oleate (SOA) and alkylphenol polyoxyethylene ether	Unmodified CuO withstand for 15 days, while modified CuO withstand for 3 months	[68]
CuO & MoS$_2$	Chemical modified palm oil	Spectral absorbency	Oleic acid	Dispersion stability of MoS$_2$ > CuO in 72 h	[72]
Graphene oxide (GO)	Paraffin oil	Sedimentation	Octadevylamine	Reduced GO precipitated after 10 days, octadevylamine reduced GO is stable even after 15 days	[88]
Graphene	350 SN base oil	Spectral absorbency	Steric and oleic acids	Evaluated by UV-vis spectrophotometer	[85]
Al$_2$O$_3$	Pure lubricating oil	Zeta potential analysis, spectral absorbency	KH-560 can hydrolyze	Without modified withstand for 20 days, while modified withstand for 50 days	[58]
ZnAl$_2$O$_4$	Pure lubricant oil	Spectral absorbency	Oleic acid	ZnAl$_2$O$_4$ modified at 70 °C had the best stability	[63]
MoS$_2$	Coconut oil & paraffin oil	Spectral absorbency	Sodium dodecyl sulfate mixed with heptane solution	Surface modified > unmodified	[76]
La(OH)$_3$/RGO	CF-4 20W-50 diesel engine oil	Sedimentation	-	Minimum precipitation occurs after 28 days	[96]
Al$_2$O$_3$/TiO$_2$	5W-30 engine oil	Spectral absorbency	Oleic acid	The dispersion stability decrease clearly after 1000 h	[110]
Cu/CNTs	Rapeseed oil	Sedimentation	Spontaneous polydopamine (PDA)	Stability of unmodified NP decrease after 12 h, modified maintain for 10 days	[102]
Ag/graphene	Paraffin oil	Spectral absorbency, sedimentation	Laser irradiation	With Laser irradiation, stability stable even after 60 days	[97]
TiO$_2$/SiO$_2$	Palm oil	Sedimentation, spectral absorbency	-	High rate sedimentation after 3 days	[100]
TiO$_2$	Water-based lubricant	Spectral absorbency	Polyethyleneimine (PEI)	After 120 h, the dispersion is stable	[56]
	Oil in water	Spectral absorbency	-	The dispersion maintain over 80% after 72 h	[67]

The sedimentation method is the easiest method to determine the stability of nanolubricants because only the observation of the nanolubricants is involved, and it is usually conducted after nanoparticles disperse in the lubricant. During the stability analysis, a photograph of the test nanolubricants is taken. However, the drawback of this method is the long duration required. Furthermore, the environmental conditions and volume should be fixed for all test samples to obtain precision results, and any relocation or disturbance has to be avoided during this analysis. The duration of this analysis is usually in the range of days to months. The dispersion stability of CuO in palm kernel oil has been researched, revealing that it fully sediments at day 16 [66]. Wu et al. reported significantly less precipitated La(OH)$_3$/RGO in diesel engine oil after 28 days [96]. A comparative study of graphite with or without dispersant in API Group III 150N base oil should be mentioned, with 1 wt% PIBISI the stability of nanolubricant remained stable for up to 50 days. In comparison, without dispersant, stability only lasts 6–7 days [81]. In contrast, including 1 wt% sorbitan monooleate as a dispersant in graphite-PAO4 lubricant, graphite fully sediments after 3 days [90]. Hence, the duration of this stability analysis is due to the different combination of lubricants and NPs, and the analysis is considered complete when the NPs fully sediment or the dispersion stability lasted for a long time.

Spectral absorbency analysis is the most efficient method to evaluate the dispersion stability of nanolubricants. Ultraviolet-visible (Uv-vis) absorption spectroscopy measurements are used in this method to characterize the stability of a variety of materials in lubricants quantitatively. This measurement is a reliable method to evaluate the dispersion stability of nanolubricants. It has

the characteristic absorption bands in the wavelength range of 190–1100 nm [122]. Xia et al. [67] reported the wavelength of absorbance of TiO_2 nanolubricant in the range of 250-500nm and maximum absorbance at 378nm. In addition, the quantitative concentration of nanofluids will be provided through this measurement, due to the linear relation of supernatant nanoparticles concentration to the absorbency [122]. Thus, this is an advantage of using this method. Furthermore, for this analysis, different test durations have been reported by researchers. Xia et al. [67] carried out the spectral absorbency analysis over 72 h for oil in water enriched with TiO_2, showing that stability is over 80%. Similarly, Gulzar et al. [72] conducted this analysis over 72 h for nanoCuO and nanoMoS$_2$ lubricant. Song et al. [63] showed the absorbance spectrum of three different temperature modified nanoZnAl$_2$O$_4$ lubricants over 140 h. A comparative study revealed the optical absorbance spectral behavior of engine oil enriched with nanocomposite Al$_2$O$_3$/TiO$_2$ in four different durations: 48, 168, 336, and 1000 h [110].

The zeta potential measurement also known as the surface charge analysis, is a technique used to determine the colloidal stability of nanoparticles. This method shows the zeta potential difference between the dispersion medium and the stern layer of fluid attached to the dispersed nanoparticle [122]. Typically, the range of zeta potential is from +100 to −100 mV, and it is related to the colloidal stability of nanolubricants. Thus, high zeta potential means electrically stabilized, while low zeta potential means dispersion instability due to the absence of a force to prevent the agglomeration of particles. In addition, if the zeta potential value is in the range of 0 to ±5mV, the particle will tend to flocculation or coagulation, and ±10 to ±30mV is considered as incipient instability. However, ±25 mV is the arbitrary value that decides the dispersion stability, in the range of ±40 to ±60 mV results in good stability, and greater than ±60 mV is excellent stability [127]. Luo et al. [58] reported that the modified Al$_2$O$_3$ nanolubricant has the average zeta potential value of 25.1 mV. The modified nanoCuO has a higher dispersion stability six times that of the unmodified nanoCuO in water [68].

7. Conclusions

Tribology is a science that has a close relationship with the development of physics. This field is already involved in the microscale and nanoscale, both of which influence lubrication, friction, wear, and sliding mechanisms. The tribological characteristics and lubrication mechanism of various types of nanoparticles as lubricant additives were reviewed here. The present review also covered the parameters of nanoparticles that affect the tribological properties, the dispersion method, techniques on enhancing dispersion stability, and nanolubricants characterization. Even though a lot of research studies have been done, the most crucial challenge is to prepare and maintain homogenous and good stability nanolubricants for a long duration. Thus, the stabilization of nanoparticles in various base oils must be investigated using multiple modification techniques.

The size, concentration, and morphology of nanoparticles are relevant to the improvement of tribological characteristics. However, the methods to determine the correlation between these factors are still lacking, but it is still promising. Besides, it is essential to discover the optimum concentration of nanoparticles in base oils. This would not only exhibit the maximum improvement but also save in terms of the cost of production. Thus, the authors recommend here the use of simulation software to optimize the concentration of nanoparticles in base oils which exhibit excellent tribological properties.

Based on the literature, there are two techniques for enhancing the dispersion stability of nanolubricants. Surface modification seems to provide more effective stabilization of nanolubricants, and it does not significantly affect the fuel properties of nanolubricants. In addition, ultrasonication is an auxiliary method in the previously mentioned techniques.

Overall, a majority of extant studies reported that nanoparticles enriched with lubricating oils improved tribological performance. The lubrication mechanism of nanoparticles cannot be fully yet understood since the mechanism is complex, and it contains various types of nanoparticles. However, for environmental protection purposes, the formulation of environmentally friendly nanolubricants is essential, which does not contain sulfur or phosphorus and will not affect the improvement of tribological properties.

References

1. Bartz, W.J. Tribology, lubricants and lubrication engineering—A review. *Wear* **1978**, *49*, 1–18. [CrossRef]
2. Mobarak, H.M.; Mohamad, E.N.; Masjuki, H.H.; Kalam, M.A.; Al Mahmud, K.A.H.; Habibullah, M.; Ashraful, A.M. The prospects of biolubricants as alternatives in automotive applications. *Renew. Sustain. Energy Rev.* **2014**, *33*, 34–43. [CrossRef]
3. Holmberg, K.; Andersson, P.; Erdemir, A. Global energy consumption due to friction in passenger cars. *Tribol. Int.* **2012**, *47*, 221–234. [CrossRef]
4. Ssempebwa, J.C.; Carpenter, D.O. The generation, use and disposal of waste crankcase oil in developing countries: A case for Kampala district, Uganda. *J. Hazard. Mater.* **2009**, *161*, 835–841. [CrossRef] [PubMed]
5. Parás, L.P.; Cortés, D.M.; Taha-Tijerina, J. Eco-friendly Nanoparticle Additives for Lubricants and Their Tribological Characterization. In *Handbook of Ecomaterials*; Martínez, L., Kharissova, O., Kharisov, B., Eds.; Springer: Cham, Switzerland, 2019; pp. 3247–3267.
6. Uflyand, I.E.; Zhinzhilo, V.A.; Burlakova, V.E. Metal-containing nanomaterials as lubricant additives: State-of-the-art and future development. *Friction* **2019**, *7*, 93–116. [CrossRef]
7. Shahnazar, S.; Bagheri, S.; Hamid, S.B.A. Enhancing lubricant properties by nanoparticle additives. *Int. J. Hydrog. Energy* **2016**, *41*, 3153–3170. [CrossRef]
8. Yu, H.L.; Yi, X.U.; Shi, P.J.; Xu, B.S.; Wang, X.L.; Qian, L.I.U. Tribological properties and lubricating mechanisms of Cu nanoparticles in lubricant. *Trans. Nonferrous Metals Soc. China* **2008**, *18*, 636–641. [CrossRef]
9. Kalin, M.; Kogovšek, J.; Remškar, M. Nanoparticles as novel lubricating additives in a green, physically based lubrication technology for DLC coatings. *Wear* **2013**, *303*, 480–485. [CrossRef]
10. Wu, Y.Y.; Tsui, W.C.; Liu, T.C. Experimental analysis of tribological properties of lubricating oils with nanoparticle additives. *Wear* **2007**, *262*, 819–825. [CrossRef]
11. Zhang, R.; Zhao, J.; Pu, J.; Lu, Z. First-Principles Investigation on the Tribological Properties of h-BN Bilayer Under Variable Load. *Tribol. Lett.* **2018**, *66*, 124. [CrossRef]
12. Huang, H.D.; Tu, J.P.; Gan, L.P.; Li, C.Z. An investigation on tribological properties of graphite nanosheets as oil additive. *Wear* **2006**, *261*, 140–144.
13. Shahmohamadi, H.; Rahmani, R.; Rahnejat, H.; Garner, C.P.; Balodimos, N. Thermohydrodynamics of lubricant flow with carbon nanoparticles in tribological contacts. *Tribol. Int.* **2017**, *113*, 50–57.
14. Meng, Y.; Su, F.; Chen, Y. Synthesis of nano-Cu/graphene oxide composites by supercritical CO_2-assisted deposition as a novel material for reducing friction and wear. *Chem. Eng. J.* **2015**, *281*, 11–19.
15. Zhang, Z.; Yu, L.; Liu, W.; Xue, Q. The effect of LaF3 nanocluster modified with succinimide on the lubricating performance of liquid paraffin for steel-on-steel system. *Tribol. Int.* **2001**, *34*, 83–88.
16. Sundus, F.; Fazal, M.A.; Masjuki, H.H. Tribology with biodiesel: A study on enhancing biodiesel stability and its fuel properties. *Renew. Sustain. Energy Rev.* **2017**, *70*, 399–412.
17. Amiri, M.; Khonsari, M.M. On the Thermodynamics of Friction and Wear—A Review. *Entropy* **2010**, *12*, 1021–1049.
18. Bruce, R.W. *Handbook of Lubrication and Tribology, Volume II*; CRC Press: Boca Raton, FL, USA, 2012; p. 1169.
19. Chan, C.-H.; Tang, S.W.; Mohd, N.K.; Lim, W.H.; Yeong, S.K.; Idris, Z. Tribological behavior of biolubricant base stocks and additives. *Renew. Sustain. Energy Rev.* **2018**, *93*, 145–157.
20. Jordan, H.; Kailyn, S.; Jason, D. Energy Education—Energy Loss. Available online: https://energyeducation.ca/encyclopedia/Energy_loss (accessed on 20 February 2020).

21.　U.S. Government. Where the Energy Goes: Gasoline Vehicles. Available online: https://www.fueleconomy.gov/feg/atv.shtml (accessed on 20 February 2020).

22.　Shafi, W.K.; Raina, A.; Haq, M.I.U. Friction and wear characteristics of vegetable oils using nanoparticles for sustainable lubrication. *Tribol. Mater. Surf. Interfaces* **2018**, *12*, 27–43.

23.　Fazal, M.A.; Haseeb, A.S.M.A.; Masjuki, H.H. Investigation of friction and wear characteristics of palm biodiesel. *Energy Convers. Manag.* **2013**, *67*, 251–256.

24.　Menezes, P.L.; Kishore; Kailas, S.V.; Lovell, M.R. Role of Surface Texture, Roughness, and Hardness on Friction During Unidirectional Sliding. *Tribol. Lett.* **2010**, *41*, 1–15.

25.　Kalin, M.; Velkavrh, I.; Vižintin, J. The Stribeck curve and lubrication design for non-fully wetted surfaces. *Wear* **2009**, *267*, 1232–1240. [CrossRef]

26.　Hamrock, B.J.; Schmid, S.R.; Jacobson, B.O. *Fundamentals of Fluid Film Lubrication*; CRC Press: Boca Raton, FL, USA, 2004.

27.　Maru, M.M.; Tanaka, D.K. Consideration of Stribeck Diagram Parameters in the Investigation on Wear and Friction Behavior in Lubricated Sliding. *J. Braz. Soc. Mech. Sci. Eng.* **2007**, *29*, 55–62. [CrossRef]

28.　Rudnick, L.R. *Synthetics, Mineral Oils, and Bio-Based Lubricants*, 2nd ed.; CRC Press: Boca Raton, FL, USA, 2013.

29.　Papay, A.G. Antiwear and Extreme-Pressure Additives in Lubricants. *Lubr. Sci.* **1998**, *10*, 209–224. [CrossRef]

30.　Rasheed, A.K.; Khalid, M.; Rashmi, W.; Gupta, T.C.S.M.; Chan, A. Graphene based nanofluids and nanolubricants—Review of recent developments. *Renew. Sustain. Energy Rev.* **2016**, *63*, 346–362. [CrossRef]

31.　American Petroleum Institute (Ed.) *Appendix E—API Base Oil Interchangeability Guidelines for Passenger Car Motoroils and Diesel Engine Oils*; American Petroleum Institute: Washington, DC, USA, 2019; pp. 1–34.

32.　Speight, J.G. Chapter 3: Hydrocarbons from Crude Oil. In *Handbook of Industrial Hydrocarbon Processes*; Elsevier: Amsterdam, The Netherlands, 2020; pp. 95–142.

33.　Stachowiak, G.W.; Batchelor, A.W. Chapter 3: Lubricants and Their Composition. In *Engineering Tribology*, 3rd ed.; Elsevier: Amsterdam, The Netherlands, 2006.

34.　Wu, M.M.; Ho, S.C.; Forbus, T.R. *Practical Advances in Petroleum Processing: Synthetic Lubricant Base Stock Processes and Products*; Springer: New York, NY, USA, 2006.

35.　Nowak, P.; Kucharska, K.; Kaminski, M. Ecological and Health Effects of Lubricant Oils Emitted into the Environment. *Int. J. Environ. Res. Public Health* **2019**, *16*, 3002. [CrossRef] [PubMed]

36.　Salimon, J.; Salih, N.; Yousif, E. Biolubricants: Raw materials, chemical modifications and environmental benefits. *Eur. J. Lipid Sci. Technol.* **2010**, *112*, 519–530. [CrossRef]

37.　Reeves, C.J.; Siddaiah, A.; Menezes, P.L. A Review on the Science and Technology of Natural and Synthetic Biolubricants. *J. Bio-Tribo-Corros.* **2017**, *3*, 1–27. [CrossRef]

38.　Dai, W.; Kheireddin, B.; Gao, H.; Liang, H. Roles of nanoparticles in oil lubrication. *Tribol. Int.* **2016**, *102*, 88–98. [CrossRef]

39.　Yang, G.; Zhang, Z.; Zhang, S.; Yu, L.; Zhang, P.; Hou, Y. Preparation and characterization of copper nanoparticles surface-capped by alkanethiols. *Surf. Interface Anal.* **2013**, *45*, 1695–1701. [CrossRef]

40.　Padgurskas, J.; Rukuiza, R.; Prosyčevas, I.; Kreivaitis, R. Tribological properties of lubricant additives of Fe, Cu and Co nanoparticles. *Tribol. Int.* **2013**, *60*, 224–232. [CrossRef]

41.　Asadauskas, S.J.; Kreivaitis, R.; Bikulčius, G.; Grigucevičienė, A.; Padgurskas, J. Tribological effects of Cu, Fe and Zn nano-particles, suspended in mineral and bio-based oils. *Lubr. Sci.* **2016**, *28*, 157–176. [CrossRef]

42.　Flores-Castañeda, M.; Camps, E.; Camacho-López, M.; Muhl, S.; García, E.; Figueroa, M. Bismuth nanoparticles synthesized by laser ablation in lubricant oils for tribological tests. *J. Alloys Compd.* **2015**, *643*, S67–S70. [CrossRef]

43.　Chou, R.; Battez, A.H.; Cabello, J.J.; Viesca, J.L.; Osorio, A.; Sagastume, A. Tribological behavior of polyalphaolefin with the addition of nickel nanoparticles. *Tribol. Int.* **2010**, *43*, 2327–2332. [CrossRef]

44.　Peng, D.X.; Yuan, K.; Chen, S.-K.; Shu, F.-C.; Chang, Y.P. Dispersion and tribological properties of liquid paraffin with added aluminum nanoparticles. *Ind. Lubr. Tribol.* **2010**, *62*, 341–348. [CrossRef]

45.　Scherge, M.; Böttcher, R.; Kürten, D.; Linsler, D. Multi-Phase Friction and Wear Reduction by Copper Nanopartices. *Lubricants* **2016**, *4*, 1–13. [CrossRef]

46.　Zhang, B.-S.; Xu, B.-S.; Xu, Y.; Gao, F.; Shi, P.-J.; Wu, Y.-X. CU nanoparticles effect on the tribological properties of hydrosilicate powders as lubricant additive for steel–steel contacts. *Tribol. Int.* **2011**, *44*, 878–886. [CrossRef]

47. Chen, Y.; Zhang, Y.; Zhang, S.; Yu, L.; Zhang, P.; Zhang, Z. Preparation of Nickel-Based Nanolubricants via a Facile In Situ One-Step Route and Investigation of Their Tribological Properties. *Tribol. Lett.* **2013**, *51*, 73–83. [CrossRef]

48. Viesca, J.L.; Battez, A.H.; González, R.; Chou, R.; Cabello, J.J. Antiwear properties of carbon-coated copper nanoparticles used as an additive to a polyalphaolefin. *Tribol. Int.* **2011**, *44*, 829–833. [CrossRef]

49. Rajubhai, V.H.; Singh, Y.; Suthar, K.; Surana, A.R. Friction and wear behavior of Al-7% Si alloy pin under pongamia oil with copper nanoparticles as additives. *Mater. Today Proc.* **2019**, *25*, 695–698. [CrossRef]

50. Shi, P.J.; Yu, H.L.; Wang, H.M.; Xu, B.S. Tribological Behaviour of Surface Modified Copper Nanoparticles as lubricating Additives. *Phys. Procedia* **2013**, *50*, 461–465. [CrossRef]

51. Wang, J.; Guo, X.; He, Y.; Jiang, M.; Sun, R. The synthesis and tribological characteristics of triangular copper nanoplates as a grease additive. *RSC Adv.* **2017**, *7*, 40249–40254. [CrossRef]

52. Zhang, S.; Hu, L.; Feng, D.; Wang, H. Anti-wear and friction-reduction mechanism of Sn and Fe nanoparticles as additives of multialkylated cyclopentanes under vacuum condition. *Vacuum* **2013**, *87*, 75–80. [CrossRef]

53. Abad, M.D.; Sánchez-López, J.C. Tribological properties of surface-modified Pd nanoparticles for electrical contacts. *Wear* **2013**, *297*, 943–951. [CrossRef]

54. Alves, S.M.; Barros, B.S.; Trajano, M.F.; Ribeiro, K.S.B.; Moura, E. Tribological behavior of vegetable oil-based lubricants with nanoparticles of oxides in boundary lubrication conditions. *Tribol. Int.* **2013**, *65*, 28–36. [CrossRef]

55. Wu, H.; Zhao, J.; Cheng, X.; Xia, W.; He, A.; Yun, J.-H.; Huang, S.; Wang, L.; Huang, H.; Jiao, S.; et al. Friction and wear characteristics of TiO_2 nano-additive water-based lubricant on ferritic stainless steel. *Tribol. Int.* **2018**, *117*, 24–38. [CrossRef]

56. Wu, H.; Zhao, J.; Xia, W.; Cheng, X.; He, A.; Yun, J.-H.; Wang, L.; Huang, H.; Jiao, S.; Huang, L.; et al. A study of the tribological behaviour of TiO_2 nano-additive water-based lubricants. *Tribol. Int.* **2017**, *109*, 398–408. [CrossRef]

57. Laad, M.; Ponnamma, D.; Sadasivuni, K.K. Tribological Studies of Nanomodified Mineral based Multi-grade Engine Oil. *Int. J. Appl. Eng. Res.* **2017**, *12*, 2855–2861.

58. Luo, T.; Wei, X.; Huang, X.; Huang, L.; Yang, F. Tribological properties of Al_2O_3 nanoparticles as lubricating oil additives. *Ceram. Int.* **2014**, *40*, 7143–7149. [CrossRef]

59. Peña-Parás, L.; Taha-Tijerina, J.; Garza, L.; Maldonado-Cortés, D.; Michalczewski, R.; Lapray, C. Effect of CuO and Al_2O_3 nanoparticle additives on the tribological behavior of fully formulated oils. *Wear* **2015**, *332–333*, 1256–1261. [CrossRef]

60. Ingole, S.; Charanpahari, A.; Kakade, A.; Umare, S.S.; Bhatt, D.V.; Menghani, J. Tribological behavior of nano TiO_2 as an additive in base oil. *Wear* **2013**, *301*, 776–785. [CrossRef]

61. Jatti, V.S.; Singh, T.P. Copper oxide nano-particles as friction-reduction and anti-wear additives in lubricating oil. *J. Mech. Sci. Technol.* **2015**, *29*, 793–798.

62. Asrul, M.; Zulkifli, N.; Masjuki, H.; Kalam, M. Tribological Properties and Lubricant Mechanism of Nanoparticle in Engine Oil. *Procedia Eng.* **2013**, *68*, 320–325. [CrossRef]

63. Song, X.; Zheng, S.; Zhang, J.; Li, W.; Chen, Q.; Cao, B. Synthesis of monodispersed $ZnAl_2O_4$ nanoparticles and their tribology properties as lubricant additives. *Mater. Res. Bull.* **2012**, *47*, 4305–4310. [CrossRef]

64. Zulkifli, N.; Kalam, M.; Masjuki, H.; Yunus, R. Experimental Analysis of Tribological Properties of Biolubricant with Nanoparticle Additive. *Procedia Eng.* **2013**, *68*, 152–157. [CrossRef]

65. Shaari, M.Z.; Roselina, N.R.N.; Kasolang, S.; Hyie, K.M.; Murad, M.C.; Abu Bakar, M.A. Investigation of Tribological Properties of Palm Oil Biolubricant Modified Nanoparticles. *J. Teknol.* **2015**, *76*, 69–73. [CrossRef]

66. Azman, N.F.; Samion, S.; Sot, M.N.H.M. Investigation of tribological properties of CuO/palm oil nanolubricant using pin-on-disc tribotester. *Green Mater.* **2018**, *6*, 30–37. [CrossRef]

67. Xia, W.; Zhao, J.; Wu, H.; Jiao, S.; Zhao, X.; Zhang, X.; Xu, J.; Jiang, Z. Analysis of oil-in-water based nanolubricants with varying mass fractions of oil and TiO_2 nanoparticles. *Wear* **2018**, *396–397*, 162–171. [CrossRef]

68. Yang, P.; Zhao, X.; Liu, Y.; Lai, X. Preparation and Tribological Properties of Dual-Coated CuO Nanoparticles as Water Based Lubricant Additives. *J. Nanosci. Nanotechnol.* **2016**, *16*, 9683–9689. [CrossRef]

69. Rabaso, P.; Ville, F.; Dassenoy, F.; Diaby, M.; Afanasiev, P.; Cavoret, J.; Vacher, B.; Le Mogne, T. Boundary lubrication: Influence of the size and structure of inorganic fullerene-like MoS_2 nanoparticles on friction and wear reduction. *Wear* **2014**, *320*, 161–178. [CrossRef]

70. Xu, Y.; Hu, E.-Z.; Hu, K.-H.; Xu, Y.; Hu, X. Formation of an adsorption film of MoS$_2$ nanoparticles and dioctyl sebacate on a steel surface for alleviating friction and wear. *Tribol. Int.* **2015**, *92*, 172–183. [CrossRef]

71. Rosentsveig, R.; Gorodnev, A.; Feuerstein, N.; Friedman, H.; Zak, A.; Fleischer, N.; Tannous, J.; Dassenoy, F.; Tenne, R. Fullerene-like MoS2 Nanoparticles and Their Tribological Behavior. *Tribol. Lett.* **2009**, *36*, 175–182. [CrossRef]

72. Gulzar, M.; Masjuki, H.; Varman, M.; Kalam, M.; Mufti, R.; Zulkifli, N.; Yunus, R.; Zahid, R. Improving the AW/EP ability of chemically modified palm oil by adding CuO and MoS2 nanoparticles. *Tribol. Int.* **2015**, *88*, 271–279. [CrossRef]

73. Zhou, L.H.; Wei, X.C.; Ma, Z.J.; Mei, B. Anti-friction performance of FeS nanoparticle synthesized by biological method. *Appl. Surf. Sci.* **2017**, *407*, 21–28. [CrossRef]

74. Wan, Q.; Jin, Y.; Sun, P.; Ding, Y. Rheological and tribological behaviour of lubricating oils containing platelet MoS$_2$ nanoparticles. *J. Nanoparticle Res.* **2014**, *16*, 2386. [CrossRef]

75. Zhang, L.L.; Tu, J.; Wu, H.; Yang, Y. WS$_2$ nanorods prepared by self-transformation process and their tribological properties as additive in base oil. *Mater. Sci. Eng. A* **2007**, *454*, 487–491. [CrossRef]

76. Koshy, C.P.; Rajendrakumar, P.K.; Thottackkad, M.V. Evaluation of the tribological and thermo-physical properties of coconut oil added with MoS$_2$ nanoparticles at elevated temperatures. *Wear* **2015**, *330–331*, 288–308. [CrossRef]

77. Kalin, M.; Kogovšek, J.; Remškar, M. Mechanisms and improvements in the friction and wear behavior using MoS$_2$ nanotubes as potential oil additives. *Wear* **2012**, *280–281*, 36–45. [CrossRef]

78. Yadgarov, L.; Petrone, V.; Rosentsveig, R.; Feldman, Y.; Tenne, R.; Senatore, A. Tribological studies of rhenium doped fullerene-like MoS2 nanoparticles in boundary, mixed and elasto-hydrodynamic lubrication conditions. *Wear* **2013**, *297*, 1103–1110. [CrossRef]

79. Peng, D.; Kang, Y.; Hwang, R.; Shyr, S.; Chang, Y. Tribological properties of diamond and SiO$_2$ nanoparticles added in paraffin. *Tribol. Int.* **2009**, *42*, 911–917. [CrossRef]

80. Raina, A.; Anand, A. Lubrication performance of synthetic oil mixed with diamond nanoparticles: Effect of concentration. *Mater. Today Proc.* **2018**, *5*, 20588–20594. [CrossRef]

81. Gupta, M.K.; Bijwe, J. A complex interdependence of dispersant in nano-suspensions with varying amount of graphite particles on its stability and tribological performance. *Tribol. Int.* **2020**, *142*, 105968. [CrossRef]

82. Sivakumar, B.; Ranjan, N.; Sundara, R.; Kamaraj, M. Tribological properties of graphite oxide derivative as nano-additive: Synthesized from the waster carbon source. *Tribol. Int.* **2020**, *142*, 105990. [CrossRef]

83. Phiri, J.; Gane, P.; Maloney, T.C. General overview of graphene: Production, properties and application in polymer composites. *Mater. Sci. Eng. B* **2017**, *215*, 9–28. [CrossRef]

84. Eswaraiah, V.; Sankaranarayanan, V.; Ramaprabhu, S. Graphene-Based Engine Oil Nanofluids for Tribological Applications. *ACS Appl. Mater. Interfaces* **2011**, *3*, 4221–4227. [CrossRef] [PubMed]

85. Lin, J.; Wang, L.; Chen, G. Modification of Graphene Platelets and their Tribological Properties as a Lubricant Additive. *Tribol. Lett.* **2010**, *41*, 209–215. [CrossRef]

86. Zhao, J.; Mao, J.; Li, Y.; He, Y.; Luo, J. Friction-induced nano-structural evolution of graphene as a lubrication additive. *Appl. Surf. Sci.* **2018**, *434*, 21–27. [CrossRef]

87. Wang, X.; Zhang, Y.; Yin, Z.; Su, Y.; Zhang, Y.; Cao, J. Experimental research on tribological properties of liquid phase exfoliated graphene as an additive in SAE 10W-30 lubricating oil. *Tribol. Int.* **2019**, *135*, 29–37. [CrossRef]

88. Vats, B.N.; Singh, M. Evaluation of tribological properties of graphene oxide dispersed paraffin oil. *Mater. Today Proc.* **2020**, *25*, 557–562. [CrossRef]

89. Chu, H.Y.; Hsu, W.C.; Lin, J.F. The anti-scuffing performance of diamond nano-particles as an oil additive. *Wear* **2010**, *268*, 960–967. [CrossRef]

90. Zhang, Z.-C.; Cai, Z.-B.; Peng, J.-F.; Zhu, M.-H. Comparison of the tribology performance of nano-diesel soot and graphite particles as lubricant additives. *J. Phys. D: Appl. Phys.* **2015**, *49*, 045304. [CrossRef]

91. Zhang, W.; Zhou, M.; Zhu, H.; Tian, Y.; Wang, K.; Wei, J.; Ji, F.; Li, X.; Li, Z.; Zhang, P.; et al. Tribological properties of oleic acid-modified graphene as lubricant oil additives. *J. Phys. D Appl. Phys.* **2011**, *44*, 4. [CrossRef]

92. Su, Y.; Gong, L.; Chen, D. An Investigation on Tribological Properties and Lubrication Mechanism of Graphite Nanoparticles as Vegetable Based Oil Additive. *J. Nanomater.* **2015**, *2015*, 1–7. [CrossRef]

93. Kiong, K.S.S.; Yusup, S.; Soon, C.V.; Arpin, T.; Samion, S.; Kamil, R.N.M. Tribological Investigation of Graphene as Lubricant Additive in Vegetable Oil. *J. Phys. Sci.* **2017**, *28*, 257–267. [CrossRef]

94. Kannan, K.T.; Rameshbabu, S. Tribological behavior of modified jojoba oil with graphene nanoparticle as additive in SAE20W40 oil using pin on disc tribometer. *Energy Sources Part A Recover. Util. Environ. Eff.* **2017**, *39*, 1842–1848. [CrossRef]

95. Zhao, J.; He, Y.; Wang, Y.; Wang, W.; Yan, L.; Luo, J. An investigation on the tribological properties of multilayer graphene and MoS2 nanosheets as additives used in hydraulic applications. *Tribol. Int.* **2016**, *97*, 14–20. [CrossRef]

96. Wu, B.; Song, H.; Li, C.; Song, R.; Zhang, T.; Hu, X. Enhanced tribological properties of diesel engine oil with Nano-Lanthanum hydroxide/reduced graphene oxide composites. *Tribol. Int.* **2020**, *141*, 105951. [CrossRef]

97. Wang, L.; Gong, P.; Li, W.; Luo, T.; Cao, B. Mono-dispersed Ag/Graphene nanocomposite as lubricant additive to reduce friction and wear. *Tribol. Int.* **2020**, *146*, 106228. [CrossRef]

98. Gan, C.; Liang, T.; Li, W.; Fan, X.; Zhu, M.-H. Amine-terminated ionic liquid modified graphene oxide/copper nanocomposite toward efficient lubrication. *Appl. Surf. Sci.* **2019**, *491*, 105–115. [CrossRef]

99. Zhang, X.; Zhu, S.; Shi, T.; Ding, H.; Bai, Y.; Di, P.; Luo, Y. Preparation, mechanical and tribological properties of WC-Al$_2$O$_3$ composite doped with graphene platelets. *Ceram. Int.* **2020**, *46*, 10457–10468. [CrossRef]

100. Gulzar, M.; Masjuki, H.H.; Kalam, M.A.; Varman, M.; Zulkifli NW, M.; Mufti, R.A.; Zahid, R.; Yunus, R. Dispersion Stability and Tribological Characteristics of TiO$_2$/SiO$_2$ Nanocomposite-Enriched Biobased Lubricant. *Tribol. Trans.* **2016**, *60*, 670–680. [CrossRef]

101. An, V.V.; Anisimov, E.; Druzyanova, V.; Burtsev, N.; Shulepov, I.A.; Khaskelberg, M. Study of tribological behavior of Cu-MoS$_2$ and Ag-MoS$_2$ nanocomposite lubricants. *SpringerPlus* **2016**, *5*, 72. [CrossRef] [PubMed]

102. Wang, Z.; Ren, R.; Song, H.; Jia, X. Improved tribological properties of the synthesized copper/carbon nanotube nanocomposites for rapeseed oil-based additives. *Appl. Surf. Sci.* **2018**, *428*, 630–639. [CrossRef]

103. Meng, Y.; Su, F.; Chen, Y. Supercritical Fluid Synthesis and Tribological Applications of Silver Nanoparticle-decorated Graphene in Engine Oil Nanofluid. *Sci. Rep.* **2016**, *6*, 31246.

104. Meng, Y.; Su, F.; Chen, Y. Effective lubricant additive of nano-Ag/MWCNTs nanocomposite produced by supercritical CO$_2$ synthesis. *Tribol. Int.* **2018**, *118*, 180–188. [CrossRef]

105. Ali, M.K.A.; Xianjun, H.; Mai, L.; Bicheng, C.; Turkson, R.F.; Qingping, C. Reducing frictional power losses and improving the scuffing resistance in automotive engines using hybrid nanomaterials as nano-lubricant additives. *Wear* **2016**, *364–365*, 270–281. [CrossRef]

106. Ataie, S.A.; Zakeri, A. Improving tribological properties of (Zn–Ni)/nano Al$_2$O$_3$ composite coatings produced by ultrasonic assisted pulse plating. *J. Alloys Compd.* **2016**, *674*, 315–322. [CrossRef]

107. Sadoun, A.; Fathy, A. Experimental study on tribological properties of Cu–Al$_2$O$_3$ nanocomposite hybridized by graphene nanoplatelets. *Ceram. Int.* **2019**, *45*, 24784–24792. [CrossRef]

108. Li, S.; Qin, H.; Zuo, R.; Bai, Z. Friction properties of La-doped Mg/Al layered double hydroxide and intercalated product as lubricant additives. *Tribol. Int.* **2015**, *91*, 60–66. [CrossRef]

109. He, Q.; Li, A.; Guo, Y.; Liu, S.; Zhang, Y.; Kong, L. Tribological properties of nanometer cerium oxide as additives in lithium grease. *J. Rare Earths* **2018**, *36*, 209–214. [CrossRef]

110. Shen, T.; Wang, D.; Yun, J.; Liu, Q.; Liu, X.; Peng, Z. Tribological properties and tribochemical analysis of nano-cerium oxide and sulfurized isobutene in titanium complex grease. *Tribol. Int.* **2016**, *93*, 332–346. [CrossRef]

111. Hou, X.; He, J.; Yu, L.; Li, Z.; Zhang, Z.; Zhang, P. Preparation and tribological properties of fluorosilane surface-modified lanthanum trifluoride nanoparticles as additive of fluoro silicone oil. *Appl. Surf. Sci.* **2014**, *316*, 515–523. [CrossRef]

112. Liu, F.; Shao, X.; Yin, Y.; Zhao, L.; Shao, Z.; Liu, X.; Meng, X. Shape controlled synthesis and tribological properties of CeVO$_4$ nanoparticles aslubricating additive. *J. Rare Earths* **2011**, *29*, 688–691. [CrossRef]

113. Lee, K.; Hwang, Y.; Cheong, S.; Choi, Y.; Kwon, L.; Lee, J.; Kim, S.H. Understanding the Role of Nanoparticles in Nano-oil Lubrication. *Tribol. Lett.* **2009**, *35*, 127–131. [CrossRef]

114. Gulzar, M.; Masjuki, H.; Kalam, M.A.; Varman, M.; Zulkifli, N.W.M.; Mufti, R.A.; Zahid, R. Tribological performance of nanoparticles as lubricating oil additives. *J. Nanoparticle Res.* **2016**, *18*, 1–25. [CrossRef]

115. Wang, X.; Yin, Y.; Zhang, G.; Wang, W.; Zhao, K. Study on Antiwear and Repairing Performances about Mass of Nano-copper Lubricating Additives to 45 Steel. *Phys. Procedia* **2013**, *50*, 466–472. [CrossRef]

116. Balaji, S.; AB, M.A.N. Tribological performance of graphene/graphite filled phenolic composites—A comparative study. *Compos. Commun.* **2019**, *15*, 34–39.

117. Liu, X.; Xu, N.; Li, W.; Zhang, M.; Chen, L.; Lou, W.; Wang, X. Exploring the effect of nanoparticle size on the tribological properties of SiO$_2$/polyalkylene glycol nanofluid under different lubrication conditions. *Tribol. Int.* **2017**, *109*, 467–472. [CrossRef]

118. Akbulut, M. Nanoparticle-Based Lubrication Systems. *J. Powder Met. Min.* **2012**, *1*, 1–3. [CrossRef]

119. Calestani, D. Characterization of the physical and chemical properties of engineered nanomaterials. In *Exposure to Engineered Nanomaterials in the Environment*; Elsevier: Amsterdam, The Netherlands, 2019; pp. 31–57.

120. Spikes, H. Friction Modifier Additives. *Tribol. Lett.* **2015**, *60*, 1–26. [CrossRef]

121. Tevet, O.; Von-Huth, P.; Popovitz-Biro, R.; Rosentsveig, R.; Wagner, H.D.; Tenne, R. Friction mechanism of individual multilayered nanoparticles. *Proc. Natl. Acad. Sci. USA* **2011**, *108*, 19901–19906. [CrossRef]

122. Yu, W.; Xie, H. A Review on Nanofluids: Preparation, Stability Mechanisms, and Applications. *J. Nanomater.* **2011**, *2012*, 1–17. [CrossRef]

123. Moshkovith, A.; Perfiliev, V.; Verdyan, A.; Lapsker, I.; Popovitz-Biro, R.; Tenne, R.; Rapoport, L. Sedimentation of IF-WS$_2$ aggregates and a reproducibility of the tribological data. *Tribol. Int.* **2007**, *40*, 117–124. [CrossRef]

124. Kołodziejczyk, Ł.; Martinez-Martinez, D.; Rojas, T.C.; Fernández, A.; Sanchez-Lopez, J. Surface-modified Pd nanoparticles as a superior additive for lubrication. *J. Nanoparticle Res.* **2006**, *9*, 639–645. [CrossRef]

125. Demas, N.G.; Timofeeva, E.V.; Routbort, J.L.; Fenske, G.R. Tribological Effects of BN and MoS$_2$ Nanoparticles Added to Polyalphaolefin Oil in Piston Skirt/Cylinder Liner Tests. *Tribol. Lett.* **2012**, *47*, 91–102. [CrossRef]

126. Gupta, M.; Bijwe, J.; Kadiyala, A.K. Tribo-Investigations on Oils with Dispersants and Hexagonal Boron Nitride Particles. *J. Tribol.* **2017**, *140*, 031801. [CrossRef]

127. Kumar, A.; Dixit, C.K. Methods for characterization of nanoparticles. In *Advances in Nanomedicine for the Delivery of Therapeutic Nucleic Acids*; Woodhead Publishing: Cambridge, UK, 2017; pp. 43–58.